

2012

# The synthesis of amphiphilic diblock copolymers: An investigation into the formation of micelles as a function of hydrophobic block length

Kevin S. Kawchak

Follow this and additional works at: <http://commons.emich.edu/theses>



Part of the [Chemistry Commons](#)

---

## Recommended Citation

Kawchak, Kevin S., "The synthesis of amphiphilic diblock copolymers: An investigation into the formation of micelles as a function of hydrophobic block length" (2012). *Master's Theses and Doctoral Dissertations*. 385.  
<http://commons.emich.edu/theses/385>

This Open Access Thesis is brought to you for free and open access by the Master's Theses, and Doctoral Dissertations, and Graduate Capstone Projects at DigitalCommons@EMU. It has been accepted for inclusion in Master's Theses and Doctoral Dissertations by an authorized administrator of DigitalCommons@EMU. For more information, please contact [lib-ir@emich.edu](mailto:lib-ir@emich.edu).

The synthesis of amphiphilic diblock copolymers: An investigation into the formation of micelles as a function of hydrophobic block length

by

Kevin S. Kawchak

Thesis

Submitted to the Department of Chemistry

Eastern Michigan University

in partial fulfillment of the requirements

for the degree of

MASTER OF SCIENCE

in

Chemistry

Thesis Committee:

Gregg Wilmes, Ph.D., Chair

Donald Snyder, Ph.D.

Jamie Scaglione, Ph.D.

March 12, 2012

Ypsilanti, Michigan

## Acknowledgements

I would like to thank the following people who have supported my graduate research activities:

Gregg Wilmes, Ph.D., Chair

Donald Snyder, Ph.D.

Jamie Scaglione, Ph.D.

Ruth Ann Armitage, Ph.D.

Heather Holmes, Ph.D.

Timothy Brewer, Ph.D.

David Arnold / Cayman Chemical

## THESIS APPROVAL FORM

The synthesis of amphiphilic diblock copolymers: An investigation into the formation of micelles as a function of hydrophobic block length

by

Kevin S. Kawchak

### **APPROVED:**

Dr. Gregg Wilmes

Thesis Chair

Dr. Donald Snyder

Committee Member

Dr. Jamie Scaglione

Committee Member

Dr. Ross Nord

Department Head

Dr. Deb deLaski-Smith

Interim Dean of the Graduate School

## ABSTRACT

Acrylate-based amphiphilic diblock copolymers show great potential for anti-cancer drug transport due to their ability to aggregate into protective core-shell micelles. Using RAFT polymerization, copolymers containing poly(acrylic acid) and poly(methyl acrylate) blocks were made with high monomer conversion and narrow distributions of molecular weight for eventual use in medicinal applications. Based on previous findings of copolymers with low weight hydrophobic blocks failing to micellize, it was hypothesized that increasing the poly(methyl acrylate) block length would allow for micelle formation. <sup>1</sup>H-NMR experiments conducted in the presence of an aqueous solution yielded diminished and broadened resonances of the lengthened hydrophobic block, which confirmed effects of micellization. As a result, a rigid hydrophobic core may be substituted with a longer flexible acrylate block for biological use. The adoption of longer core chain lengths in a micellar system may be useful in other transport applications when precipitation of drugs in vivo remains an issue.

## TABLE OF CONTENTS

Acknowledgements.....	ii
Approval.....	iii
Abstract.....	iv
List of Tables.....	vii
List of Figures.....	viii
Chapter 1: Introduction.....	1
Copolymers and Micelle Formation.....	1
Amphiphilic Copolymer Medicinal Applications.....	2
Reversible Addition Fragmentation chain Transfer (RAFT) Polymerization.....	3
<sup>1</sup> H-NMR/ <sup>13</sup> C-NMR (Nuclear Magnetic Resonance).....	6
E-HSQC (Edited-Heteronuclear Single Quantum Correlation) NMR.....	6
Size Exclusion Chromatography (SEC).....	7
Justification and Hypothesis.....	7
Chapter 2: Experimental.....	8
Chain Transfer Agent (CTA) Materials.....	8
CTA-1 <i>tert</i> -butyl dodecyl carbanotrithioate.....	8
CTA-2 2-(((dodecylthio)carbonothioyl)thio)-2-methylpropanoic acid.....	9
Polymer Materials.....	11
Poly( <i>tert</i> -butyl acrylate)/Poly(methyl acrylate).....	11
Poly( <i>tert</i> -butyl acrylate- <i>b</i> -methyl acrylate)/Poly(methyl acrylate- <i>b</i> - <i>tert</i> -butyl acrylate)..	13
Poly(acrylic acid- <i>b</i> -methyl acrylate)/Poly(methyl acrylate- <i>b</i> -acrylic acid).....	14
Polymer Characterization.....	14
Micellization Experiments.....	16

Chapter 3: Results and Discussion.....	20
CTA-1 <i>tert</i> -butyl dodecyl carbanotrithioate <sup>1</sup> H-NMR.....	20
CTA-1 <i>tert</i> -butyl dodecyl carbanotrithioate <sup>13</sup> C-NMR.....	21
Poly( <i>tert</i> -butyl acrylate) <sup>1</sup> H-NMR.....	22
Poly( <i>tert</i> -butyl acrylate) <sup>13</sup> C-NMR.....	23
Poly(methyl acrylate) Percent Conversion <sup>1</sup> H-NMR.....	24
Poly( <i>tert</i> -butyl acrylate) SEC.....	25
Poly( <i>tert</i> -butyl acrylate- <i>b</i> -methyl acrylate) <sup>1</sup> H-NMR.....	26
Poly( <i>tert</i> -butyl acrylate- <i>b</i> -methyl acrylate) <sup>13</sup> C-NMR.....	27
Diblock Copolymer Percent Conversion <sup>1</sup> H-NMR.....	28
Poly(methyl acrylate- <i>b-tert</i> -butyl acrylate) SEC.....	29
Poly(acrylic acid- <i>b</i> -methyl acrylate) E-HSQC NMR.....	30
Poly(acrylic acid- <i>b</i> -methyl acrylate) <sup>13</sup> C-NMR.....	32
Poly(methyl acrylate- <i>b</i> -acrylic acid) (66- <i>b</i> -60) <sup>1</sup> H-NMR.....	33
Poly(acrylic acid- <i>b</i> -methyl acrylate) (65- <i>b</i> -194) <sup>1</sup> H-NMR.....	34
Chapter 4: Conclusions.....	36
References.....	38
Appendix A.....	45
Appendix B.....	45

## LIST OF TABLES

<u>Table</u>		<u>Page</u>
1	CTA-1 Chain Transfer Agent Reagents.....	9
2	CTA-2 Chain Transfer Agent Reagents.....	10
3	Homopolymer Conditions and Results.....	17
4	Diblock Copolymer Conditions and Results.....	18
5	Amphiphilic Copolymer Conditions and Results.....	19



## LIST OF FIGURES

<u>Figure</u>		<u>Page</u>
1	Reversible Addition Fragmentation chain Transfer (RAFT) Polymerization.....	5
2	CTA-1 Chain Transfer Agent Synthesis.....	9
3	CTA-2 Chain Transfer Agent Synthesis.....	10
4	Homopolymer Synthesis.....	12
5	Diblock Copolymer Synthesis.....	13
6	Amphiphilic Diblock Copolymer Synthesis.....	14
7	CTA-1 <i>tert</i> -butyl dodecyl carbanotrithioate <sup>1</sup> H-NMR.....	20
8	CTA-1 <i>tert</i> -butyl dodecyl carbanotrithioate <sup>13</sup> C-NMR.....	21
9	HPT-6 poly( <i>tert</i> -butyl acrylate) <sup>1</sup> H-NMR.....	22
10	HPT-6 poly( <i>tert</i> -butyl acrylate) <sup>13</sup> C-NMR.....	23
11	HPM-13 poly(methyl acrylate) Conversion <sup>1</sup> H-NMR.....	24
12	HPT-5 poly( <i>tert</i> -butyl acrylate) SEC.....	25
13	DTM-4 poly( <i>tert</i> -butyl acrylate- <i>b</i> -methyl acrylate) <sup>1</sup> H-NMR.....	26
14	DTM-4 poly( <i>tert</i> -butyl acrylate- <i>b</i> -methyl acrylate) <sup>13</sup> C-NMR.....	27
15	Diblock Percent Conversion Second Monomer <sup>1</sup> H-NMR.....	28
16	DMT-1 poly(methyl acrylate- <i>b</i> - <i>tert</i> -butyl acrylate) SEC.....	29
17	DAC-1 poly(acrylic acid- <i>b</i> -methyl acrylate) E-HSQC NMR.....	31
18	DAC-1 poly(acrylic acid- <i>b</i> -methyl acrylate) <sup>13</sup> C-NMR.....	32
19	DMA-6 poly(methyl acrylate- <i>b</i> -acrylic acid) (66- <i>b</i> -60) <sup>1</sup> H-NMR.....	33
20	DAC-1 poly(acrylic acid- <i>b</i> -methyl acrylate) (65- <i>b</i> -194) 25% D <sub>2</sub> O <sup>1</sup> H-NMR.....	35
21	DAC-1 poly(acrylic acid- <i>b</i> -methyl acrylate) (65- <i>b</i> -194) 75% D <sub>2</sub> O <sup>1</sup> H-NMR.....	35

## Chapter 1: Introduction

### Copolymers and Micelle Formation

Polymers are macromolecular chains consisting of many subunits that are formed by consecutive additions of monomer. Diblock copolymers, in particular, have two characteristic subunit types in a single non-repeating AB pattern.<sup>1-3</sup> Amphiphilic diblock copolymers consist of two regions with substantially different solubility properties. For example, a polymer composed of a hydrophobic poly(methyl acrylate) and a hydrophilic poly(acrylic acid) block can aggregate into micellar structures upon introduction to an aqueous solution.<sup>4</sup> In this fashion, the hydrophobic region of the amphiphilic molecule initiates micellization by collapsing to form the core, while the hydrophilic block forms a protective shell.<sup>5</sup>

Smaller surfactant molecules used as detergents and emulsifiers have long been studied in determining the size, shape, and physical properties of various micelles.<sup>6-7</sup> Relatively high concentrations of surfactants have been observed for micelle formation.<sup>8</sup> The concentration at which a block copolymer achieves micellization is referred to as the critical aggregation concentration (CAC). Copolymers are more ideal for micellar applications than surfactants due to decreased CAC requirements.<sup>9</sup> Lower copolymer concentrations necessary for micelle formation were determined to be a function of dispersion, hydrogen bonding, and electrostatic intermolecular forces associated with the hydrophobic block.<sup>10-12</sup>

When the CAC is reached for a copolymer, small polymeric micelles form. The micelles then coalesce as local concentrations of copolymer are further increased.<sup>13-14</sup> Micelle dissolution can then be triggered by a change in temperature, pH, salt concentration, or light intensity.<sup>15-16</sup> Assembly and disassembly of the micelle structure is necessary for delivery device function.

The glass transition temperature ( $T_g$ ) is a useful indicator for a polymer's physical properties at a given temperature. The  $T_g$  provides information on the reversible transition of a polymer from a brittle to molten state.<sup>17</sup> Therefore, the relative chain stiffness related by the  $T_g$  is believed to have a large effect on the polymer's ability to form micelles.<sup>18</sup> Copolymer block types containing less rigid acrylate substitutions have a lower  $T_g$ , which is historically favored for shell blocks.<sup>19</sup> Micellization due to hydrophobic block collapse is less likely for acrylate core types due to the lack of an alpha methyl substitution.

### **Amphiphilic Copolymer Medicinal Applications**

Solubility differences within biological transport devices allow for hydrophobic molecular transport to exist. For instance, physiologically occurring transporters such as low/high density lipoproteins (LDL/HDL) contain a water soluble shell with a hydrophobic core analogous to the synthetic amphiphilic micelle.<sup>20</sup> Micelles have been proposed as a transport device for a variety of proteins, genes, and pharmaceuticals with a low therapeutic index.<sup>21-22</sup> In addition, encapsulating drugs with relatively low lethal concentrations above the therapeutic effect provides additional flexibility in drug design. Polymeric micelles generally exhibit slow rates of dissolution in vitro, allowing for retention of loaded drugs for a longer time period, which could translate into higher accumulations of drug at a potential target site. For receptor mediated drug delivery, hydrophilic shell end cap moieties such as sugar molecules and peptides could be attached to target a biological response.<sup>1-3, 23-24</sup>

Non-bonding methods to entrap lipophilic molecules within the hydrophobic core have also been employed. For example, a solution of water, cisplatin, and poly(ethylene glycol-*b*-aspartic acid) yielded micelles containing the anti-tumor drug.<sup>25-28</sup>

Entrapped doxorubicin has also been found to increase micelle stabilization and prolong the release of both bonded and entrapped medicine in vitro.<sup>29</sup> Re-uptake into the mononuclear phagocyte system (MPS) while in the blood stream remains a primary obstacle in designing micellar systems resistant to non-selective attack. Attempts are currently being made to optimize micelle size and hydrophilic block density in order to resist MPS attack.<sup>30</sup>

### **Reversible Addition Fragmentation chain Transfer (RAFT) Polymerization**

Reversible addition fragmentation chain transfer (RAFT) is a controlled radical polymerization technique. RAFT polymerizations are typically performed in a solution of monomer, chain transfer agent (CTA), and initiator.<sup>31</sup> Ratios of monomer:CTA and CTA:initiator control the degree of polymerization ( $D_p$ ) and, hence, the molecular weight.<sup>32</sup> Reactant ratios are optimized in consideration of viscosity, rate of polymerization, and the initiating species. Initiation occurs at higher temperatures in which a radical initiator such as 2,2'-Azobis(2-methylpropionitrile) (AIBN) forms two equivalents of radical species. The radicals formed from the initiator commence chain growth with the addition of monomer. The CTA interrupts polymerization during the monomer addition process. In addition, the CTA tertiary alkyl group can initiate monomer as a result of chain transfer processes. Polymer radicals undergoing chain transfer reversibly form CTA-terminated polymer in the process of increasing chain length, as seen in Figure 1. Chain equilibrium also occurs when two growing polymer chains exchange the terminal CTA.<sup>33</sup> The decreased rate of propagation due to chain transfer processes yields polymers with a relatively narrow distribution of molecular weights.<sup>34-36</sup> As polymerization is complete, RAFT polymers characteristically contain pendant CTA moieties.

Solution polymerization of RAFT block copolymers requires monomer, homopolymer, AIBN, and solvent. A homopolymer:AIBN ratio is used analogous to the initial CTA:AIBN homopolymer reaction to make copolymer with a desired molecular weight ( $M_n$ ).<sup>37-38</sup> Reversible chain transfer between the growing diblock chain and the CTA occurs to suspend polymerization. In addition, CTA equilibrium between two diblock chains limits the dispersity of the second block. Diblock copolymers are prone to radical side reactions, as any radical species can add directly to the second monomer type to form new homopolymer.<sup>39</sup> Additional purification steps are taken to remove oligomeric impurities caused by the undesired radical reactions. Due to solubility issues of polymerizing a highly hydrophilic block directly, a post-polymerization reaction such as de-esterification of *tert*-butyl ester groups to carboxylic acids may be used to achieve the amphiphilic diblock copolymer product.<sup>40-41</sup>

End group conjugation on either the hydrophobic or hydrophilic blocks will potentially play a role in the ability of the copolymer to function as a drug delivery device. Terminal isopropyl cyano groups derived from AIBN can be used in a variety of organic reactions including nucleophilic addition, nucleophilic acyl substitution, and nitrile hydrolysis.<sup>42-44</sup> Terminal CTA moieties can be reduced to a thiol in yielding an attachment site for biological motifs or possibly used for polymeric grafting or multi-arm star synthesis.<sup>45-47</sup> Other CTAs can be implemented to perform reactions at benzyl, carboxylic acid, and cyano sites.<sup>48-49</sup> Acrylic acid moieties have also been used to allow for multiple medicine attachments. Although doxorubicin has been tested extensively with side chains moieties, drugs such as mitomycin C, mitoxantrone, and paclitaxel have also been associated with carboxyl substituted cores.<sup>50</sup>

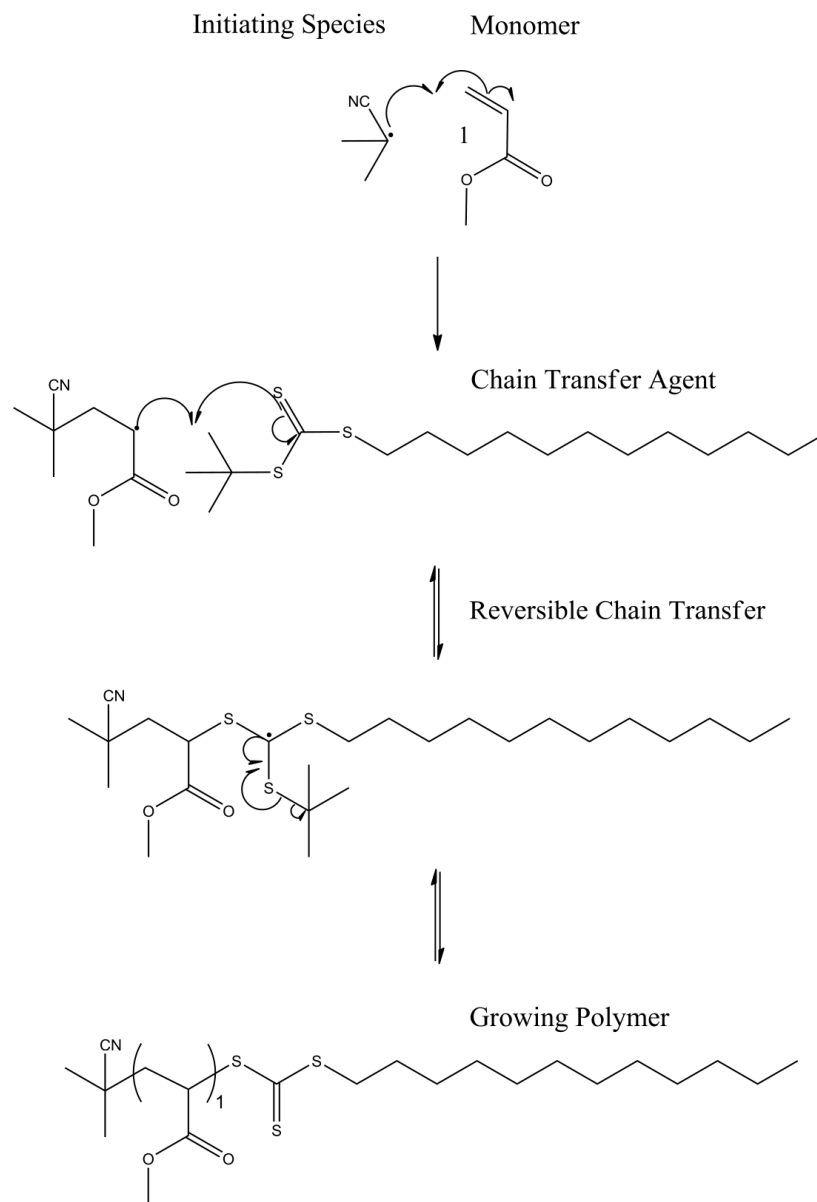


**Figure 1.** Reversible Addition Fragmentation chain Transfer (RAFT) Polymerization

## **$^1\text{H-NMR}/^{13}\text{C-NMR}$ (Nuclear Magnetic Resonance)**

$^1\text{H-NMR}$  and  $^{13}\text{C-NMR}$  spectra are useful for verifying the presence of CTA resonances in RAFT copolymers. With low molecular weight oligomers, CTA resonances are more prominent due to a low monomer:CTA ratio. The chemical shifts of particular monomer and polymer peaks are also readily observed in  $^1\text{H-NMR}$ . Spectral peak intensities provide information regarding the relative amounts of monomer and polymer present.<sup>51</sup> In general, polymer proton resonances appear upfield from monomer protons due to the shielding effect of randomly coiled macromolecular structures. The chemical environment of each monomer residue is influenced by the stereochemistry of several adjacent neighboring functional groups.<sup>52</sup> Therefore, a larger range of methine and methylene resonances is observed in both  $^1\text{H}$  and  $^{13}\text{C}$  spectra for non-stereospecific RAFT polymers. Theoretical molecular weights for de-esterified RAFT copolymers determined by the monomer:CTA and second monomer:hompolymer ratios are verified by monomer conversion in  $^1\text{H-NMR}$ , and also with  $^{13}\text{C}$  carbonyl integrations for each block type. Effects of micellization can be observed with NMR spectroscopy by the presence of diminished resonances from hydrophobic block protons.

## **E-HSQC (Edited-Heteronuclear Single Quantum Correlation) NMR**

The two dimensional  $^1\text{H-}^{13}\text{C}$  E-HSQC NMR (Edited-Heteronuclear Single Quantum Correlation) experiment is useful for providing polymer and solvent correlations when peak overlap exists. The F2 axis displays proton resonances that can be correlated to the F1  $^{13}\text{C}$  axis. Because E-HSQC NMR is a  $^1\text{H}$  detected method, sensitivity advantages in obtaining phasing information over the traditional  $^{13}\text{C}$  DEPT 135 experiment exist. CH, CH<sub>2</sub>, and CH<sub>3</sub> information included with the 2D plot are obtained with shorter collection times than in alternative 1D experiments.

## Size Exclusion Chromatography (SEC)

Size Exclusion Chromatography (SEC) provides peak intensities as a function of retention time. Larger molecules are preferentially excluded from the column and reach the detector first.<sup>53</sup> The exclusionary method provides better separation with shorter experiment times in comparison to traditional columns.<sup>54</sup> In addition, the presence of multimodal distributions from side reactions can be observed with homopolymer and diblock copolymer sample analysis.<sup>55</sup> Polydispersity indices close to 1 indicate a relatively narrow distribution of chain lengths. Chain growth as a function of reaction time can be monitored by obtaining chromatographs at multiple reaction time points. The monomer:CTA and second monomer: homopolymer ratios can be used in approximating values for  $D_p$  when multi-detector SEC is not available.

## Justification and Hypothesis

The RAFT polymerization method yields acrylate polymers of uniform molecular weight, which is desirable for medicinal applications. Previous group studies focused on synthesizing amphiphilic block copolymers with a rigid methacrylate core block that appeared to form micelles when analyzed in  $^1\text{H-NMR}$  experiments. It was determined that micellization did not occur for polymers with low  $M_n$  flexible blocks. The purpose of this study was to determine whether a non-micellar diblock copolymer with a low molecular weight hydrophobic acrylate block could be synthesized differently to form useful macroscopic structures. Two additional objectives of the study were to achieve efficient monomer conversion and predictable molecular weights. The hypothesis of the study was that increasing the core block length on a diblock copolymer would improve the effects of micellization when introduced into an aqueous environment due to additional hydrophobic intermolecular forces of the acrylate chains.



## Chapter 2: Experimental

### Chain Transfer Agent (CTA) Materials

Carbon disulfide ( $\text{CS}_2$ ,  $\geq 99.9\%$ ), tripotassium phosphate ( $\text{K}_3\text{PO}_4$ ,  $\geq 98\%$ ), 1-dodecanethiol ( $\geq 98\%$ ), 2-bromoisobutyric acid (98%), *tert*-butyl thiol (99%), and 1-bromododecane (97%) were purchased from Sigma-Aldrich. The following chemicals were purchased from various manufacturers: acetone (Macron Chemicals,  $\geq 99.5\%$ ), dichloromethane (DCM, EMD Chemicals, 99.5%), hexanes (Fischer Chemical, 99.9%), ethyl acetate (Fischer Chemical, 99.9%), hydrochloric acid (Fischer Chemical, 37.3%), and chloroform-*d* (Cambridge Isotope Laboratories, 0.03% TMS, 99.8%).

### CTA-1 *tert*-butyl dodecyl carbanotrithioate

CTA synthesis was followed according to procedures provided by Skey et al.<sup>48</sup> Equimolar amounts of *tert*-butyl thiol and  $\text{K}_3\text{PO}_4$  were added to acetone and allowed to stir for 10 minutes (Table 1).  $\text{CS}_2$  was added to the tertiary alkyl thiolate solution (Figure 2). 1-bromododecane was then added to the solution, forming a KBr precipitate. The solution was allowed to stir for 10 hours at room temperature, and the precipitate was removed by suction filtration. The precipitate was washed with acetone, and the solvent was removed from the product under reduced pressure. The crude product was dissolved in hexanes and purified by column chromatography on silica gel to remove the 1-bromododecane reagent. The product was collected with ethyl acetate, and the solvent was removed under reduced pressure to yield a bright orange solid. The reaction was subsequently scaled up three-fold.

$^1\text{H-NMR}$  (chloroform- $d$ )  $\delta$  3.24-3.28 (S-CH<sub>2</sub>-(CH<sub>2</sub>)<sub>10</sub>CH<sub>3</sub>), 1.62 (S-C(CH<sub>3</sub>)<sub>3</sub>), 1.22-1.42 (S-CH<sub>2</sub>-(CH<sub>2</sub>)<sub>10</sub>CH<sub>3</sub>), 0.84-0.88 (S-CH<sub>2</sub>-(CH<sub>2</sub>)<sub>10</sub>CH<sub>3</sub>),  $^{13}\text{C-NMR}$  (chloroform- $d$ )  $\delta$  224.0 (S-C=S-S), 54.2(S-C(CH<sub>3</sub>)<sub>3</sub>), 36.2 (S-CH<sub>2</sub>-(CH<sub>2</sub>)<sub>10</sub>CH<sub>3</sub>), 28.0-34.0 (S-CH<sub>2</sub>-(CH<sub>2</sub>)<sub>10</sub>CH<sub>3</sub>), 22.8 (S-C(CH<sub>3</sub>)<sub>3</sub>), 14.2 (S-CH<sub>2</sub>-(CH<sub>2</sub>)<sub>10</sub>CH<sub>3</sub>).

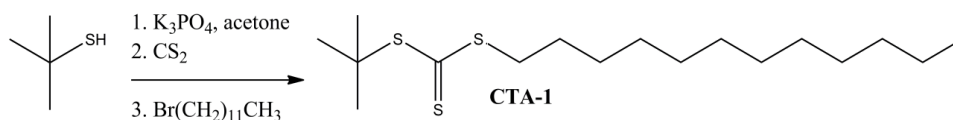


**Figure 2.** CTA-1 Chain Transfer Agent Synthesis

**Table 1.** CTA-1 Chain Transfer Agent Reagents

CTA	<i>tert</i> -butyl thiol	K <sub>3</sub> PO <sub>4</sub>	CS <sub>2</sub>	1-bromododecane	acetone	Yield	Percent Yield
CTA-1 <sub>i</sub>	1.20 mL	2.61 g	0.7 mL	2.8 mL	20 mL	3.10 g	84.2%
CTA-1	3.80 mL	7.07 g	6.0 mL	8.0 mL	60 mL	7.48 g	67.5%

### CTA-2 2-(((dodecylthio)carbonothioyl)thio)-2-methylpropanoic acid

Equimolar amounts of dodecane thiol and K<sub>3</sub>PO<sub>4</sub> were added to acetone and allowed to stir for 10 minutes (Table 2). An excess of CS<sub>2</sub> was added to the primary alkyl thiolate solution. Equimolar 2-bromoisobutyric acid was then added to the solution, forming a KBr precipitate. The solution was allowed to stir overnight at room temperature, and the precipitate was removed by suction filtration. The precipitate was washed with acetone, and the solvent was removed under reduced pressure. The residue was extracted with dichloromethane twice and washed with HCl, water, and brine. The solvent was removed from the residue, and the crude product was dissolved in ethyl acetate and purified by column chromatography with ethyl acetate on silica gel to remove residual reagent. The product shown in Figure 3 was removed from solvent under reduced pressure to yield a bright yellow solid.

$^1\text{H-NMR}$  (chloroform- $d$ )  $\delta$  11.0 (COOH not observed) 3.25-3.30 (S-CH $_2$ -(CH $_2$ ) $_{10}$ CH $_3$ ), 1.91-1.94 (S-CH $_2$ -CH $_2$ -(CH $_2$ ) $_9$ CH $_3$ ), 1.71-1.74 (S-C(CH $_3$ ) $_2$ COOH), 1.15-1.44 (S-(CH $_2$ ) $_2$ -(CH $_2$ ) $_9$ CH $_3$ ), 0.83-0.92 (S-(CH $_2$ ) $_{11}$ -CH $_3$ ),  $^{13}\text{C-NMR}$  (chloroform- $d$ )  $\delta$  226.2 (S-C=S-S not observed), 178.1 (COOH), 55.6 (S-C(CH $_3$ ) $_2$ COOH), 37.1 (S-CH $_2$ -(CH $_2$ ) $_{10}$ CH $_3$ ), 32.0 (S-CH $_2$ -CH $_2$ -(CH $_2$ ) $_9$ CH $_3$ ), 27.8-29.8 (S-(CH $_2$ ) $_2$ -(CH $_2$ ) $_8$ -CH $_2$ -CH $_3$ ), 25.3 (S-C(CH $_3$ ) $_2$ COOH), 22.8 (S-(CH $_2$ ) $_{10}$ CH $_2$ -CH $_3$ ), 14.2 (S-(CH $_2$ ) $_{11}$ -CH $_3$ ).

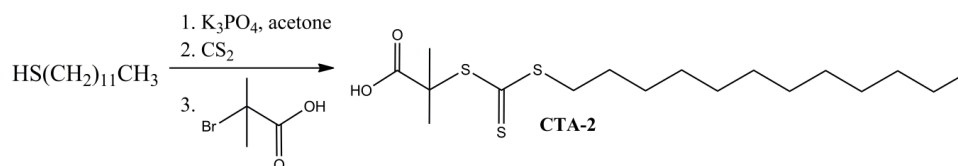


**Figure 3.** CTA-2 Chain Transfer Agent Synthesis

**Table 2.** CTA-2 Chain Transfer Agent Reagents

CTA	1-dodecanethiol	K $_3$ PO $_4$	CS $_2$	2-bromoisobutyric acid	acetone	Yield	Percent Yield
CTA-2	1.60 mL	1.27 g	1.1 mL	1.05 g	20 mL	1.98 g	90.7%

## Polymer Materials

2,2'-Azobis(2-methylpropionitrile) (AIBN, 98%), methyl acrylate (100 ppm MEHQ inhibitor, 99%), *tert*-butyl acrylate (10-20 ppm MEHQ inhibitor, 98%), and trifluoroacetic acid (TFA, 99%) were purchased from Sigma-Aldrich. AIBN was recrystallized from methanol. The following solvents were purchased from various manufacturers: dichloromethane (DCM, EMD Chemicals, 99.5%), methanol (VDW, 99.8%), hexanes (Fischer Chemical, 99.9%), benzene (Sigma-Aldrich,  $\geq 99.9\%$ ; Alfa Aesar,  $\geq 99.5\%$ ), tetrahydrofuran (THF, EMD chemicals, 250 ppm BHT inhibitor, 99.2%), chloroform-d (Cambridge Isotope Laboratories, 0.03% TMS, 99.8%), dimethyl sulfoxide-d<sub>6</sub> (DMSO-d<sub>6</sub> Cambridge Isotope Laboratories, 99.9%), 1,4-dioxane-d<sub>8</sub> (Cambridge Isotope Laboratories, 99%), and D<sub>2</sub>O (Cambridge Isotope Laboratories, 99.9%). THF was distilled from sodium and benzophenone for inhibitor removal.

## Poly(*tert*-butyl acrylate)/Poly(methyl acrylate)

Homopolymer reactions (Figure 4) were prepared in a similar manner to Chiefari et al.<sup>31</sup> In general, the solution viscosity was dependent on the concentration of monomer (Appendix A). The monomer:CTA ratio and CTA:AIBN ratio were varied to achieve desired molecular weights. Polymers with a variety of molecular weights were synthesized for use in potential micellization experiments. A summary of poly(methyl acrylate) and poly(*tert*-butyl acrylate) reactions performed are listed in Table 3.

General polymerization procedure: A benzene solution of AIBN was injected into a 50-mL Schlenk flask. The CTA solid was then added to the reaction vessel. Additional benzene was added to the vessel by syringe to achieve the desired volume. Either methyl acrylate or *tert*-butyl acrylate was passed through a pipet column of alumina gel to remove the MEHQ inhibitor.

The monomer was then added to the flask, and the solution was degassed twice by freeze-pump-thaw cycling over liquid N<sub>2</sub>. Most reactions proceeded as a 5-25 mL solution under a stream of nitrogen gas in an oil bath at 80 ± 5°C. Reaction times generally did not exceed 24 hours and varied depending on the experiment type. In addition, aliquots were removed at time intervals in some experiments for further study of monomer conversion and molecular weights of growing chains. Polymerized reactions were removed from solution under reduced pressure and redissolved in minimal amounts of benzene. A selection of poly(methyl acrylate) samples were precipitated into cold hexanes. The majority of poly(*tert*-butyl acrylate) samples were precipitated into 9:1 to 99:1 methanol:water solutions.

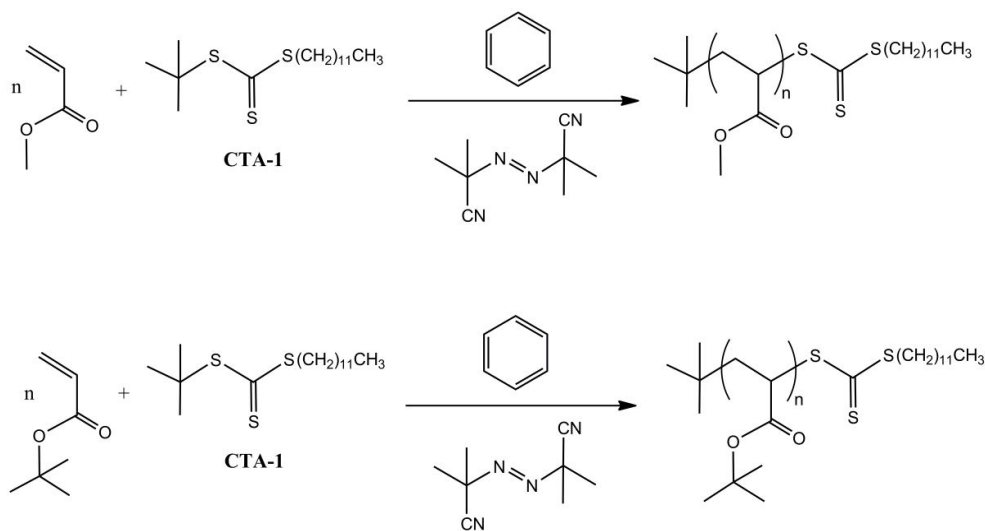


**Figure 4.** Homopolymer Synthesis

## Poly(*tert*-butyl acrylate-*b*-methyl acrylate)/Poly(methyl acrylate-*b*-*tert*-butyl acrylate)

Diblock copolymer reactions were performed with a 5:1 homopolymer:AIBN ratio (Figure 5). Factors affecting viscosity and rate of monomer conversion were similar to homopolymer reactions, as highlighted in Appendix B. Degree of polymerizations for diblock copolymers were obtained from the second monomer:homopolymer ratio and confirmed by  $^1\text{H-NMR}$ . A summary of acrylate copolymer reactions performed are listed in Table 4.

General polymerization procedure: A benzene solution of AIBN was injected into a 25-mL Schlenk flask. The homopolymer was then added to the reaction vessel followed with the desired volume of benzene added by syringe. Either *tert*-butyl acrylate or methyl acrylate was run through a pipet column of alumina gel to remove the MEHQ inhibitor. The monomer was added to the container, and the solution was degassed twice using freeze-pump-thaw cycling over liquid  $\text{N}_2$ . Most reactions occurred as a 5-20 mL solution under a stream of  $\text{N}_2$  gas in an oil bath at  $80 \pm 5^\circ\text{C}$  for approximately 24 hours.

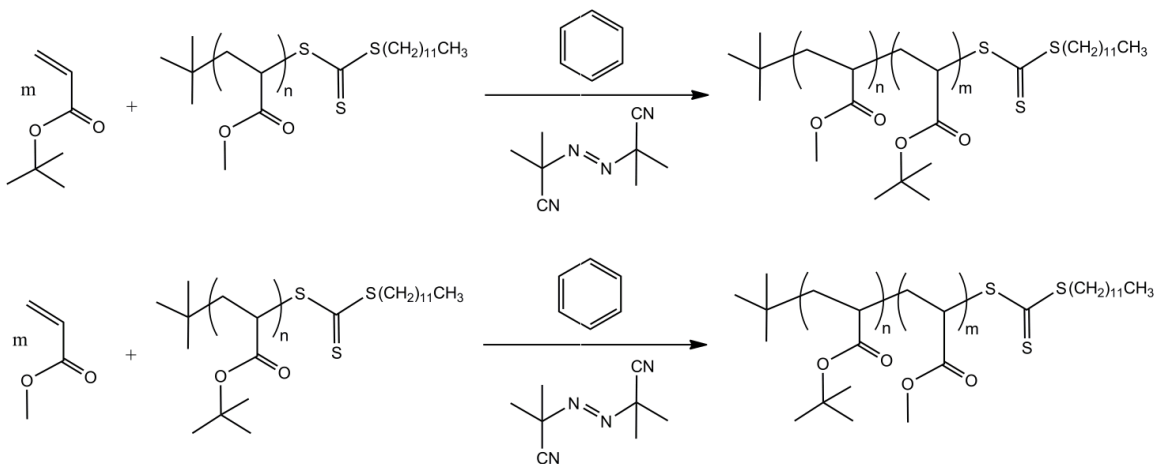


**Figure 5.** Diblock Copolymer Synthesis

## Poly(acrylic acid-*b*-methyl acrylate)/Poly(methyl acrylate-*b*-acrylic acid)

A de-esterification reaction in a solution of trifluoroacetic acid and methylene chloride afforded the synthesis of poly(acrylic acid) from poly(*tert*-butyl acrylate) blocks as shown in Figure 6. A 5:1 TFA:*tert*-butyl acrylate unit ratio was used, and the solution was allowed to stir at room temperature overnight. The solvent was removed under reduced pressure. Either poly(acrylic acid-*b*-methyl acrylate) or poly(methyl acrylate-*b*-acrylic acid) copolymers were precipitated in hexanes to afford the purified amphiphilic diblock copolymer product. A summary of copolymer reactions performed are listed in Table 5.

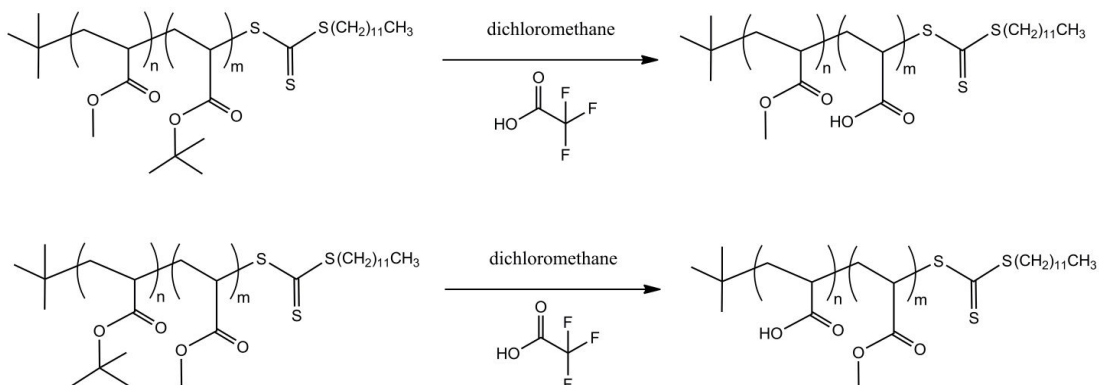


**Figure 6.** Amphiphilic Diblock Copolymer Synthesis

## Polymer Characterization

NMR sample preparations: 10 mg/mL samples of either homopolymer or non-hydrolyzed diblock samples in chloroform-*d* were prepared in an NMR tube. Amphiphilic copolymer samples were prepared in either DMSO-*d*<sub>6</sub> or 1,4-dioxane-*d*<sub>8</sub>. Gradient shimming with 16-128 <sup>1</sup>H scans was performed on the samples using a JEOL 400MHz NMR spectrometer. For <sup>13</sup>C experiments, an average of 7000 scans with a 5 second relaxation delay was used to obtain spectra. Data processing was performed using the manufacturer's Delta v4.3.6 software.

In addition to product verification,  $^1\text{H}$ -NMR was used to determine the rate of monomer conversion for both homopolymer and diblock copolymer samples. For polymerizing samples in solution, 50  $\mu\text{L}$  aliquots were extracted at various time intervals. Percent conversion was calculated based on the number of monomer protons and polymer protons present for a given monomer type. For conversion of methyl acrylate to poly(methyl acrylate), the monomer vinyl protons were divided by the sum of monomer methyl ester and poly(methyl ester) protons. For conversion of *tert*-butyl acrylate to poly(*tert*-butyl acrylate), the monomer vinyl protons were divided by 1/3 (the sum of monomer *tert*-butyl ester and poly(*tert*-butyl ester) protons). In general, molecular weights were approximated using  $^1\text{H}$  and  $^{13}\text{C}$  resonances to verify that block ratios were analogous to either the monomer:CTA or second monomer:homopolymer ratio.

2D  $^1\text{H}$ - $^{13}\text{C}$  correlations were obtained using E-HSQC (Edited-Heteronuclear Single Quantum Correlation) NMR with a 30 mg/mL sample of DAC-1 poly(acrylic acid-*b*-methyl acrylate) in 25%  $\text{D}_2\text{O}$ /75% 1,4-dioxane- $\text{d}_8$ . High resolution  $^1\text{H}$ -NMR and  $^{13}\text{C}$ -NMR spectra were obtained for the x and y projections on the plot. CH,  $\text{CH}_2$ , and  $\text{CH}_3$  phasing information was also included as part of the edited, pulsed gradient sequence to assist in distinguishing multiple solvent resonances.

SEC sample preparation: 4 mg/mL samples of either homopolymer or non-hydrolyzed copolymer were prepared in THF. The solvent was sonicated prior to collection for 10 minutes. A Shimadzu LC-20AT with a SPD-M20A detector and a Tosoh M0049-903K GPC column were used to obtain chromatographs of samples. An Agilent 1100 HPLC with a G1315A detector, autosampler, and the Tosoh GPC column were also used for acquiring molecular weight data. Either poly(methyl methacrylate) or poly(styrene) standards were analyzed on days of collection for calibration.



20  $\mu\text{L}$  samples were run for 15 minutes at a 1 mL/min solvent flow rate to obtain chromatographs. Molecular weights were obtained using Polymer Laboratory's Cirrus software package. Some  $D_p$  values obtained for poly(*tert*-butyl acrylate) blocks were found to be large overestimates of the monomer:CTA or second monomer:homopolymer ratio, and thus spectroscopic methods were used to estimate chain length.

### **Micellization Experiments**

A 2.5 mg/mL sample of DMA-6 poly(methyl acrylate-*b*-acrylic acid) (66-*b*-60) (SEC- $^1\text{H-NMR}$ ) and DAC-1 poly(acrylic acid-*b*-methyl acrylate) (65-*b*-194) in varying ratios of solvent were analyzed by  $^1\text{H-NMR}$  micellization experiments. Samples with higher concentrations of 1,4-dioxane- $\text{d}_8$  than  $\text{D}_2\text{O}$  were considered to be present in a hydrophobic environment. Concentrations of  $\text{D}_2\text{O}$  were then raised in samples to simulate an aqueous milieu. The hydrophobic block resonances of DMA-6 and DAC-1 were compared to observe diminishing or broadening effects of micellization due to the hydrophobic block chain length upon increasing  $\text{D}_2\text{O}$  concentrations.

**Table 3.** Homopolymer Conditions and Results

poly(methyl acrylate) experiments

Polymer ID	Mon:CTA <sup>a</sup>	[Mon]	CTA:AIBN	CTA ID	Temp <sup>b</sup> (°C)	Yield	Percent Recovery	Reaction Time
HPM-1	398:1	2.0 M	5.0:1	CTA-1	84.6	3491 mg	66.3% <sup>c</sup>	210 min
HPM-2	381:1	1.0 M	5.1:1	CTA-2	80.0	2346 mg	89.5%	1350 min
HPM-3	297:1	2.0 M	5.0:1	CTA-1	81.0	2615 mg	49.9% <sup>c</sup>	210 min
HPM-4	194:1	2.0 M	4.4:1	CTA-2	83.0	2039 mg	19.3% <sup>c</sup>	300 min
HPM-5	191:1	1.0 M	5.0:1	CTA-2	80.0	685 mg	19.4% <sup>c</sup>	1200 min
HPM-6	188:1	2.0 M	5.3:1	CTA-1	83.9	3050 mg	57.8% <sup>c</sup>	210 min
HPM-7	184:1	4.0 M	5.4:1	CTA-1	83.2	7014 mg	66.4% <sup>c</sup>	210 min
HPM-8	151:1	4.0 M	5.1:1	CTA-1 <sub>i</sub>	75.0	8016 mg	N.D. <sup>d</sup>	Overnight
HPM-9	151:1	2.0 M	5.7:1	CTA-1 <sub>i</sub>	75.0	4203 mg	N.D. <sup>d</sup>	Overnight
HPM-10	98:1	2.0 M	5.1:1	CTA-1	81.0	2868 mg	53.2% <sup>c</sup>	210 min
HPM-11	98:1	2.0 M	4.9:1	CTA-2	75.0	2333 mg	64.7%	Overnight
HPM-12	97:1	4.0 M	5.1:1	CTA-1	83.2	6640 mg	61.6% <sup>c</sup>	210 min
HPM-13	82:1	2.1 M	4.4:1	CTA-1 <sub>i</sub>	79.0	3013 mg	79.8%	Overnight
HPM-14	80:1	2.1 M	5.1:1	CTA-1 <sub>i</sub>	80.0	2121 mg	56.2%	1440 min
HPM-15	78:1	2.0 M	5.1:1	CTA-1	82.5	4159 mg	N.D. <sup>d</sup>	210 min
HPM-16	76:1	2.1 M	4.9:1	CTA-1 <sub>i</sub>	76.9	2749 mg	72.6%	1440 min
HPM-17	66:1	2.0 M	4.7:1	CTA-2	75.0	2955 mg	40.4%	1200 min
HPM-18	40:1	2.0 M	5.0:1	CTA-1	82.5	572 mg	20.0% <sup>c</sup>	210 min
HPM-19	25:1	2.0 M	5.1:1	CTA-1 <sub>i</sub>	75.0	3377 mg	60.2%	Overnight
HPM-20	24:1	2.0 M	4.5:1	CTA-1 <sub>i</sub>	75.0	3485 mg	61.8%	Overnight

poly(*tert*-butyl acrylate) experiments

Polymer ID	Mon:CTA <sup>a</sup>	[Mon]	CTA:AIBN	CTA ID	Temp <sup>b</sup> (°C)	Yield	Percent Recovery	Reaction Time
HPT-1	199:1	2.0 M	5.0:1	CTA-1	81.8	3291 mg	42.2% <sup>c</sup>	210 min
HPT-2	198:1	4.0 M	5.1:1	CTA-1	81.6	3145 mg	20.2% <sup>c</sup>	210 min
HPT-3	98:1	4.0 M	5.1:1	CTA-2	81.6	2595 mg	16.4% <sup>c</sup>	210 min
HPT-4	90:1	2.0 M	11:1	CTA-2	70.0	674 mg	21.1%	30 min
HPT-5	81:1	2.0 M	4.5:1	CTA-1 <sub>i</sub>	83.0	4225 mg	79.6% <sup>c</sup>	360 min
HPT-6	65:1	4.0 M	5.0:1	CTA-1	79.5	3936 mg	73.6%	180 min

<sup>a</sup> Average measured homopolymer PDI = 1.20, range = 1.003-1.65<sup>b</sup> Temperature of oil bath<sup>c</sup> <sup>1</sup>H-NMR monomer conversion/SEC molecular weight sampling<sup>d</sup> Final mass recorded prior to removal of residual solvent

**Table 4.** Diblock Copolymer Conditions and Resultspoly(methyl acrylate-*b*-*tert*-butyl acrylate) experiments

Polymer ID	Mon: pma <sup>a</sup>	[Mon]	pma: AIBN	CTA ID	pma ID	Temp <sup>b</sup> (°C)	Yield	Percent Recovery	Reaction Time
DMT-1	412:1	2.0 M	5.0:1	CTA-1	HPM-6	83.9	3492 mg	54.6% <sup>c</sup>	180 min
DMT-2	188:1	0.87 M	2.1:1	CTA-2	HPM-11	75.0	642 mg	73.6%	Overnight
DMT-3	179:1	1.1 M	1.4:1	CTA-2	HPM-17	75.0	653 mg	70.1%	Overnight
DMT-4	151:1	3.1 M	6.3:1	CTA-1 <sub>i</sub>	HPM-8	75.0	19649 mg	N.D. <sup>d</sup>	1440 min
DMT-5	151:1	1.6 M	6.3:1	CTA-1 <sub>i</sub>	HPM-9	75.0	8421 mg	N.D. <sup>d</sup>	1440 min
DMT-6	100:1	0.87 M	1.2:1	CTA-2	HPM-11	75.0	1046 mg	N.D. <sup>d</sup>	Overnight
DMT-7	74:1	0.97 M	6.0:1	CTA-1 <sub>i</sub>	HPM-14	79.8	3651 mg	72.5% <sup>c</sup>	1510 min
DMT-8	60:1	1.1 M	1.4:1	CTA-2	HPM-17	75.0	737 mg	43.7%	Overnight
DMT-9	53:1	0.89 M	2.3:1	CTA-2	HPM-11	75.0	512 mg	35.5%	Overnight
DMT-10	52:1	0.84 M	5.7:1	CTA-1 <sub>i</sub>	HPM-19	70.0	1396 mg	85.2%	Overnight
DMT-11	25:1	0.84 M	7.1:1	CTA-1 <sub>i</sub>	HPM-19	70.0	1611 mg	77.9%	Overnight
DMT-12	12:1	0.84 M	7.3:1	CTA-1 <sub>i</sub>	HPM-19	70.0	2375 mg	75.4%	Overnight

poly(*tert*-butyl acrylate-*b*-methyl acrylate) experiments

Polymer ID	Mon: pma <sup>a</sup>	[Mon]	pma: AIBN	CTA ID	pma ID	Temp <sup>b</sup> (°C)	Yield	Percent Recovery	Reaction Time
DTM-1	439:1	4.0 M	5.0:1	CTA-1	HPT-2	77.1	1797 mg	74.0%	120 min
DTM-2	213:1	4.0 M	5.0:1	CTA-2	HPT-3	77.1	904 mg	58.4% <sup>c</sup>	120 min
DTM-3	213:1	4.0 M	5.0:1	CTA-2	HPT-3	77.1	387 mg	32.9% <sup>c</sup>	120 min
DTM-4	194:1	4.0 M	5.0:1	CTA-1	HPT-6	83.2	1654 mg	54.9%	120 min
DTM-5	82:1	1.4 M	5.0:1	CTA-1 <sub>i</sub>	HPT-5	77.8	4476 mg	63.0% <sup>c</sup>	480 min

<sup>a</sup> Average measured diblock copolymer PDI = 1.29, Range = 1.20-1.40<sup>b</sup> Temperature of oil bath<sup>c</sup> <sup>1</sup>H-NMR monomer conversion/SEC molecular weight sampling<sup>d</sup> Final mass recorded prior to removal of residual solvent

**Table 5.** Amphiphilic Copolymer Conditions and Resultspoly(methyl acrylate-*b*-acrylic acid) experiments

Polymer ID	pma:ptba	CTA ID	Block ID	DCM	Temp (°C)	Yield	Percent Recovery	Time
DMA-1	151:151	CTA-1 <sub>i</sub>	DMT-4	50 mL	rt	16600 mg	84.7%	Overnight
DMA-2	151:151	CTA-1 <sub>i</sub>	DMT-5	50 mL	rt	7358 mg	87.4%	Overnight
DMA-3	98:188	CTA-2	DMT-2	20 mL	rt	246 mg	54.8%	Overnight
DMA-4	98:179	CTA-2	DMT-3	20 mL	rt	216 mg	48.1%	Overnight
DMA-5	66:60	CTA-2	DMT-8	20 mL	rt	263 mg	80.4%	Overnight
DMA-6	66:60	CTA-2	DMT-8	20 mL	rt	741 mg	N.D. <sup>a</sup>	Overnight
DMA-7	25:52	CTA-1 <sub>i</sub>	DMT-10	25 mL	rt	1049 mg	75.1%	Overnight
DMA-8	25:25	CTA-1 <sub>i</sub>	DMT-11	25 mL	rt	1665 mg	N.D. <sup>a</sup>	Overnight
DMA-9	25:12	CTA-1 <sub>i</sub>	DMT-12	25 mL	rt	2019 mg	85.0%	Overnight

poly(acrylic acid-*b*-methyl acrylate) experiments

Polymer ID	ptba:pma	CTA ID	Block ID	DCM	Temp (°C)	Yield	Percent Recovery	Time
DAC-1	65:194	CTA-1	DTM-4	10 mL	rt	1413 mg	85.4%	Overnight

<sup>a</sup> Final mass recorded prior to removal of residual solvent

## Chapter 3: Results and Discussion

### CTA-1 *tert*-butyl dodecyl carbanotrithioate $^1\text{H-NMR}$

Chemical shifts and coupling information obtained for CTA-1 were verified with values reported by Skey et al.<sup>48</sup> Distinguishable resonances included the dodecyl alpha methylene peak at 3.26 ppm (2H, triplet), as well as the *tert*-butyl peak at 1.62 ppm (9H, singlet) shown in Figure 7. The remaining dodecyl methylene protons appeared at 1.20-1.42 ppm (20H, broad), with the terminal methyl at 0.87 ppm (3H, triplet). In general, the  $^1\text{H-NMR}$  for CTA-1 was monitored for the consumption of reactants during polymerization. The synthesis of CTA-1 was preferred over CTA-2 because of the favorable  $\text{S}_{\text{N}}2$  reaction with 1-bromododecane over the analogous  $\text{S}_{\text{N}}1$  reaction with 2-bromoisobutyric acid.

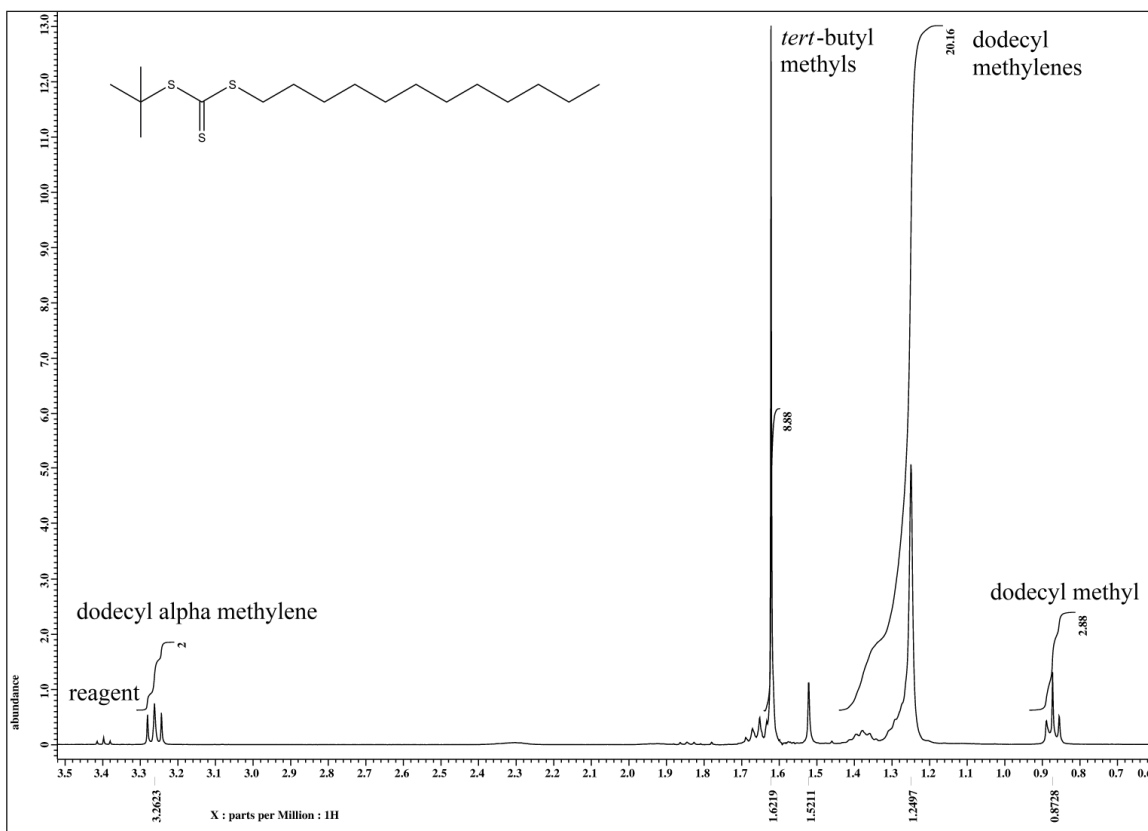
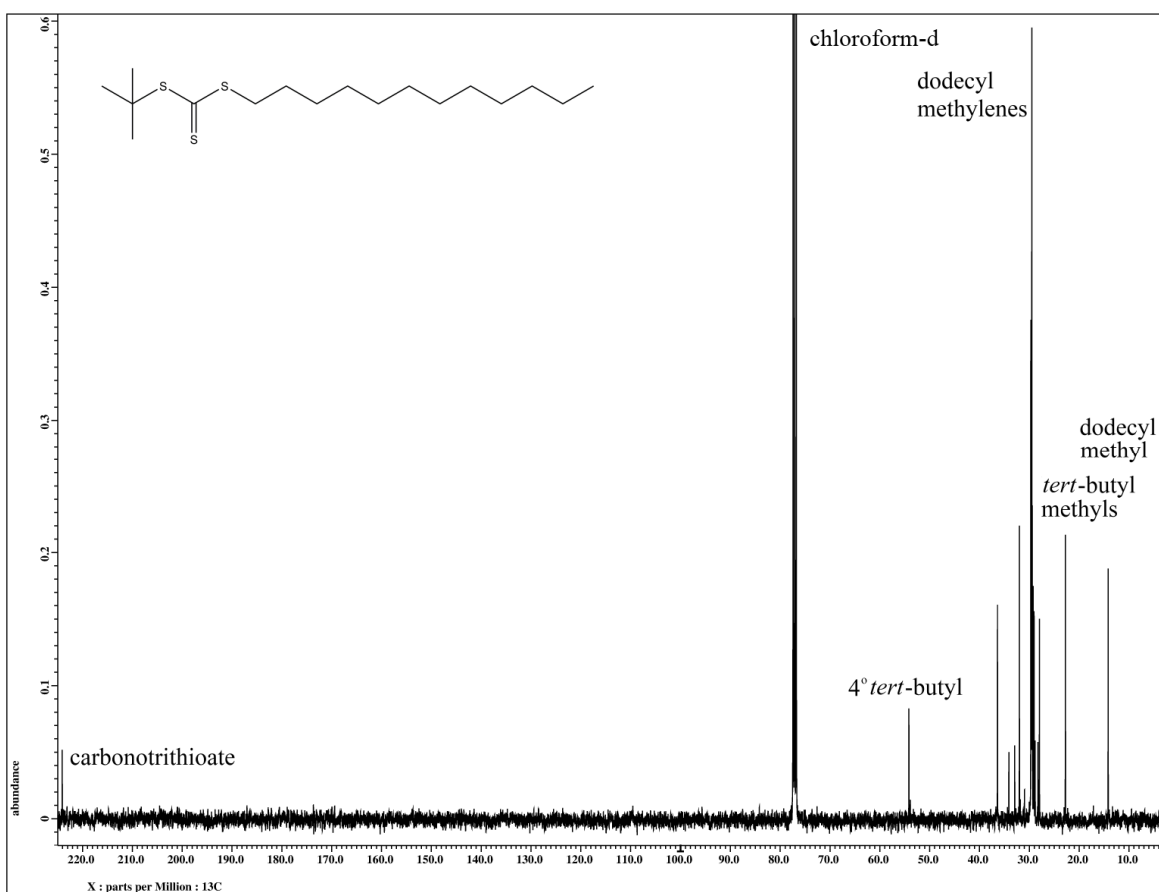


Figure 7. CTA-1 *tert*-butyl dodecyl carbanotrithioate  $^1\text{H-NMR}$

## CTA-1 *tert*-butyl dodecyl carbanotrithioate $^{13}\text{C}$ -NMR

The structure of CTA-1 was confirmed by  $^{13}\text{C}$ -NMR with the carbanotrithioate carbon peak at 224.0 ppm. The peak at 54.2 ppm represented the quaternary *tert*-butyl carbon. The dodecyl alpha methylene peak at 36.4 ppm was readily apparent due to its proximity to the electron withdrawing carbanotrithioate functional group. The remaining dodecyl methylene carbon resonances were present at 28.0-34.0 ppm. The *tert*-butyl methyls at the 22.5 ppm peak were downfield from the dodecyl methyl. The dodecyl  $\text{CH}_3$  resonance was apparent at 14.2 ppm, as depicted in Figure 8.



**Figure 8.** CTA-1 *tert*-butyl dodecyl carbanotrithioate  $^{13}\text{C}$ -NMR

## Poly(*tert*-butyl acrylate) <sup>1</sup>H-NMR

The <sup>1</sup>H-NMR of HPT-6 poly(*tert*-butyl acrylate) contained regions of overlap between polymer backbone protons, *tert*-butyl ester protons, and also CTA-1 dodecyl methylenes. A correlation was made between the methine (1H) backbone proton with the methylene (2H) and *tert*-butyl (9H) protons. The 1:11 ratio closely reflected the integration ratios apparent in Figure 9. A proton integration ratio of 1:11.27 methine: (methylene + *tert*-butyl) for this polymer was a good approximation without accounting for CTA resonance overlap. For smaller block sizes, CTA resonances were more prominently overlapped with the poly(*tert*-butyl ester) resonances.

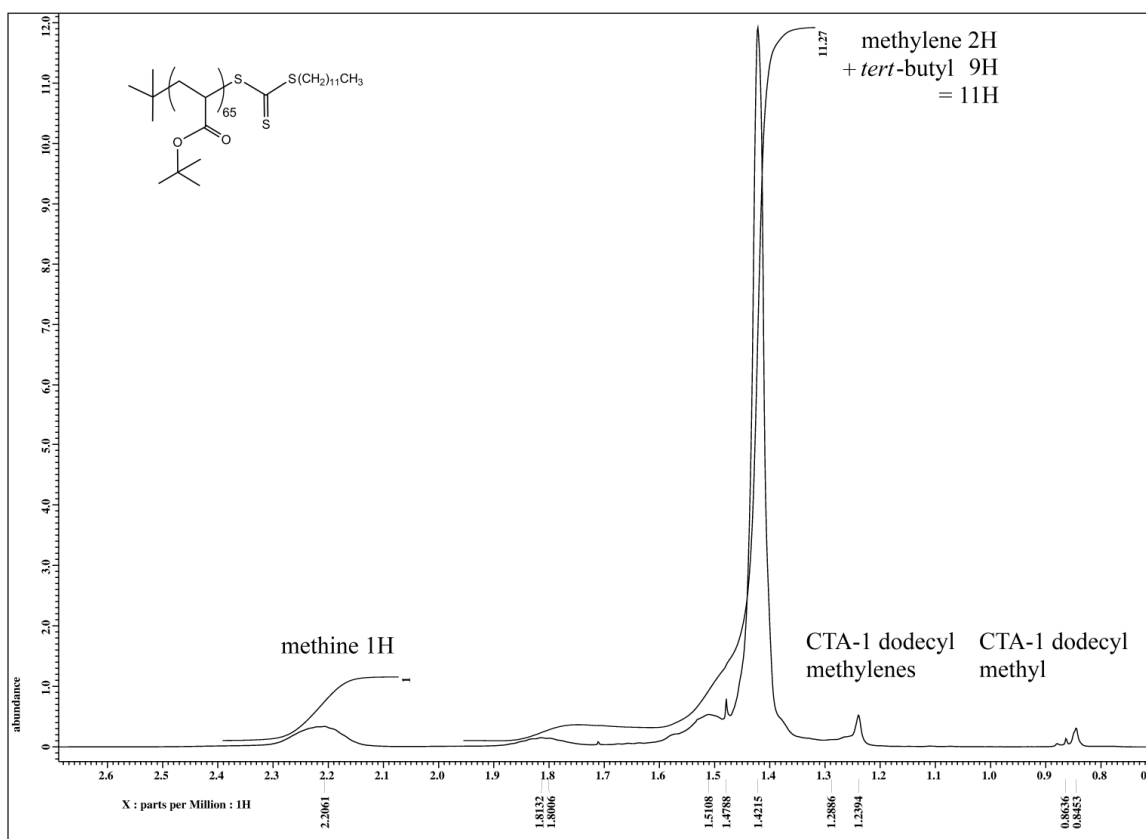


**Figure 9.** HPT-6 poly(*tert*-butyl acrylate) <sup>1</sup>H-NMR

## Poly(*tert*-butyl acrylate) $^{13}\text{C}$ -NMR

The  $^{13}\text{C}$ -NMR spectrum of HPT-6 assisted in verifying the presence of the ester carbonyl peak at 174.0 ppm. The  $4^\circ$  *tert*-butyl carbon peak was present at 80.5 ppm. The methine resonances at 42.0 and 42.1 ppm indicated the various stereochemistries of monomer repeat units on the homopolymer chain. In addition, the methylene resonances at 35.9 and 37.2 ppm were very broad due to the relative stereochemistry on each methylene repeat unit. The Figure 10 insert shows the effect of neighboring repeat units evident with both HPT-6 methine and methylene carbons. The peak for the *tert*-butyl ester methyls was also apparent at 28.0 ppm.

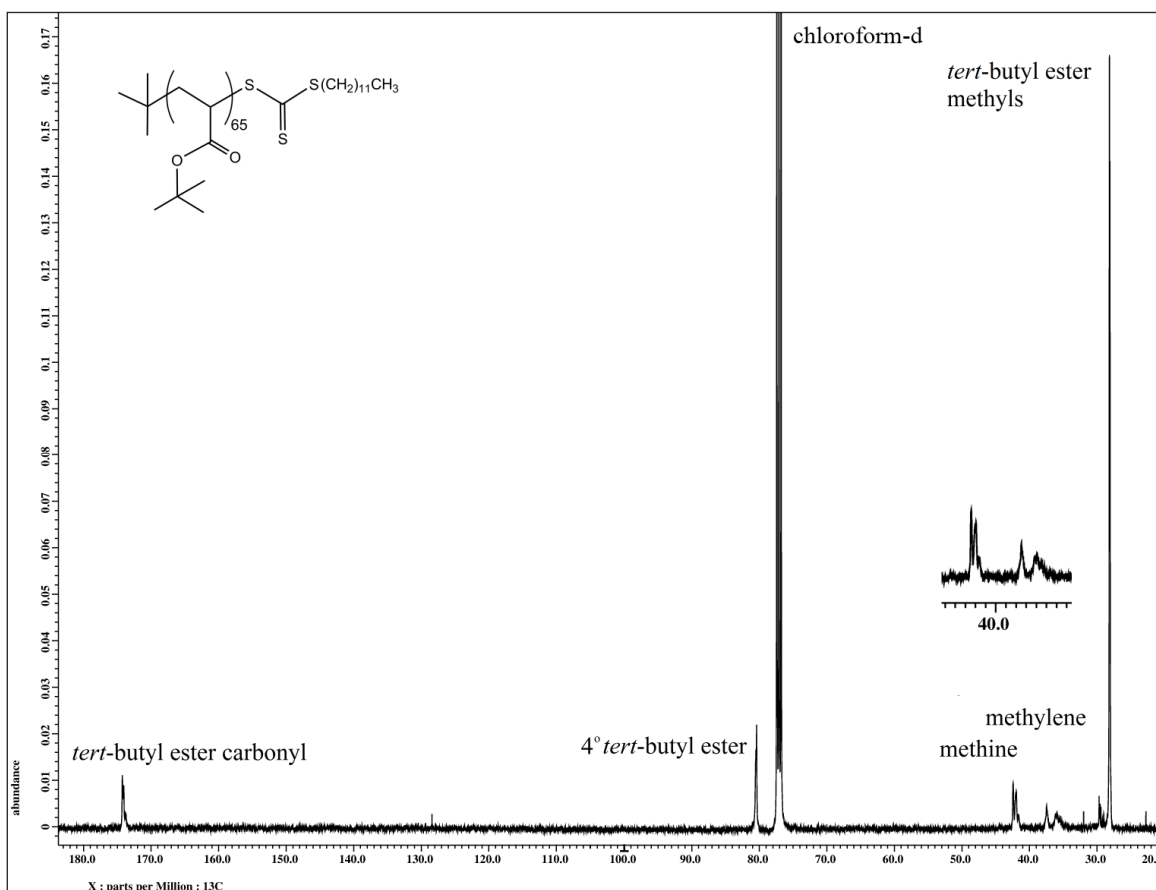
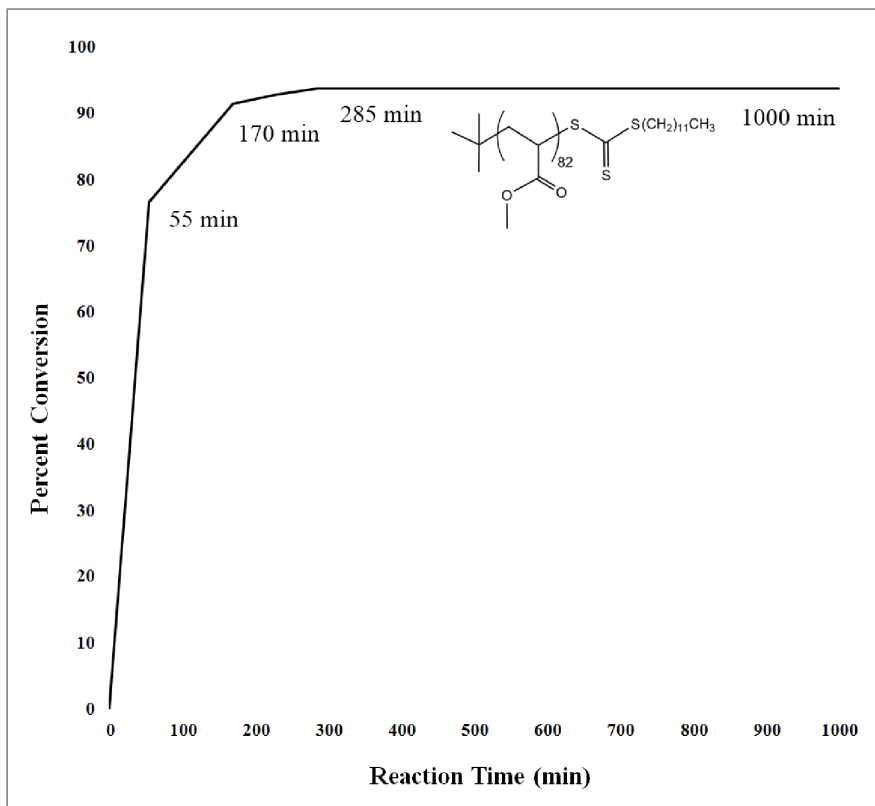


Figure 10. HPT-6 poly(*tert*-butyl acrylate)  $^{13}\text{C}$ -NMR



## Poly(methyl acrylate) Percent Conversion $^1\text{H-NMR}$

A kinetic experiment to determine the percent conversion of methyl acrylate to poly(methyl acrylate) as a function of polymerization time was conducted. Poly(*tert*-butyl acrylate) had similar rates of conversion when compared to poly(methyl acrylate), but overlap with poly(*tert*-butyl ester) methyls, backbone protons, and CTA peaks in  $^1\text{H-NMR}$  made this polymer difficult to interpret. The RAFT system was generally efficient, with high percent conversion being based off of the methyl acrylate vinylic protons divided by the total number of methyl ester protons. Figure 11 shows a 94.7% conversion within 5 hours of polymerizing the HPM-13 sample. Additional polymerization time past 5 hours yielded, in some cases, lower molecular weight. In homopolymer experiments, kinetic data suggested that an initial refractory period may exist, in which no polymerization is observed.



**Figure 11.** HPM-13 poly(methyl acrylate) Conversion  $^1\text{H-NMR}$

## Poly(*tert*-butyl acrylate) SEC

Molecular weight data as a function of reaction time obtained by SEC for HPT-5 poly(*tert*-butyl acrylate) illustrated the monomodal distribution of RAFT systems. Throughout polymerization, molecular weight ( $M_n$ ) increased gradually and was represented by a decrease in elution time. An exception with some polymerizations to these general findings was the presence of an initial refractory period, depicted at 60 min in Figure 12. The cause of low molecular weight chains at low reaction times was most likely due to an excess of chain transfer processes over propagation. In general, after the presence of any refractory period, polymer was formed at molecular weights reflected by the monomer:CTA ratio.

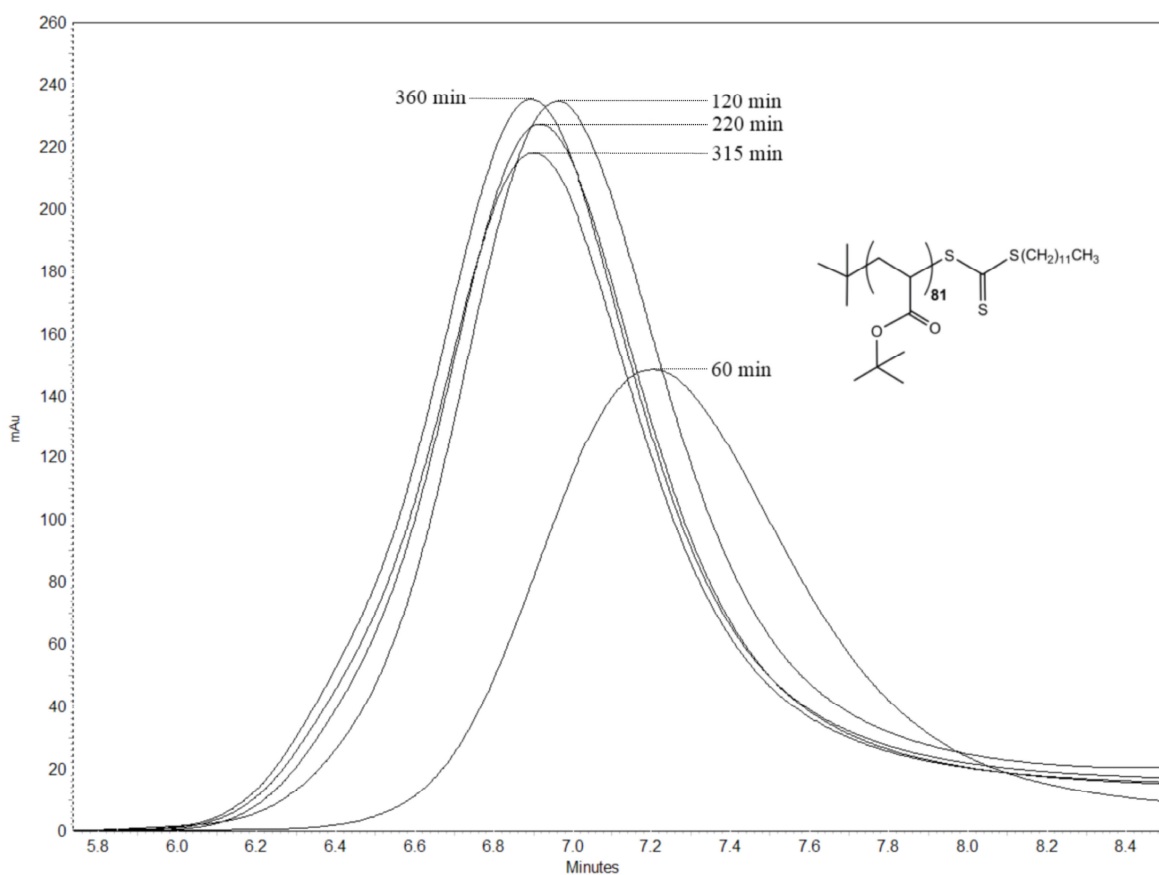


**Figure 12.** HPT-5 poly(*tert*-butyl acrylate) SEC

## Poly(*tert*-butyl acrylate-*b*-methyl acrylate) <sup>1</sup>H-NMR

Verification of poly(*tert*-butyl acrylate-*b*-methyl acrylate) formation was marked by the appearance of a poly(methyl ester) peak at 3.64 ppm, as seen in Figure 13. In addition, <sup>1</sup>H-NMR integration ratios of DTM-4 were verified with the monomer:(homopolymer units) ratio.

In the DTM-4 sample, both methylene types and *tert*-butyl methyl resonances were severely overlapped, which was not ideal for verifying product formation. The theoretical methyl ester resonance: methine poly(*tert*-butyl acrylate) + methine poly(methyl acrylate) yields 2.25:1, or 3H (194) : (1H (194) + 1H (65)). The NMR integration yielded 2.17:1, or 3:1.38; which was a good indication that the desired diblock copolymer size was formed.

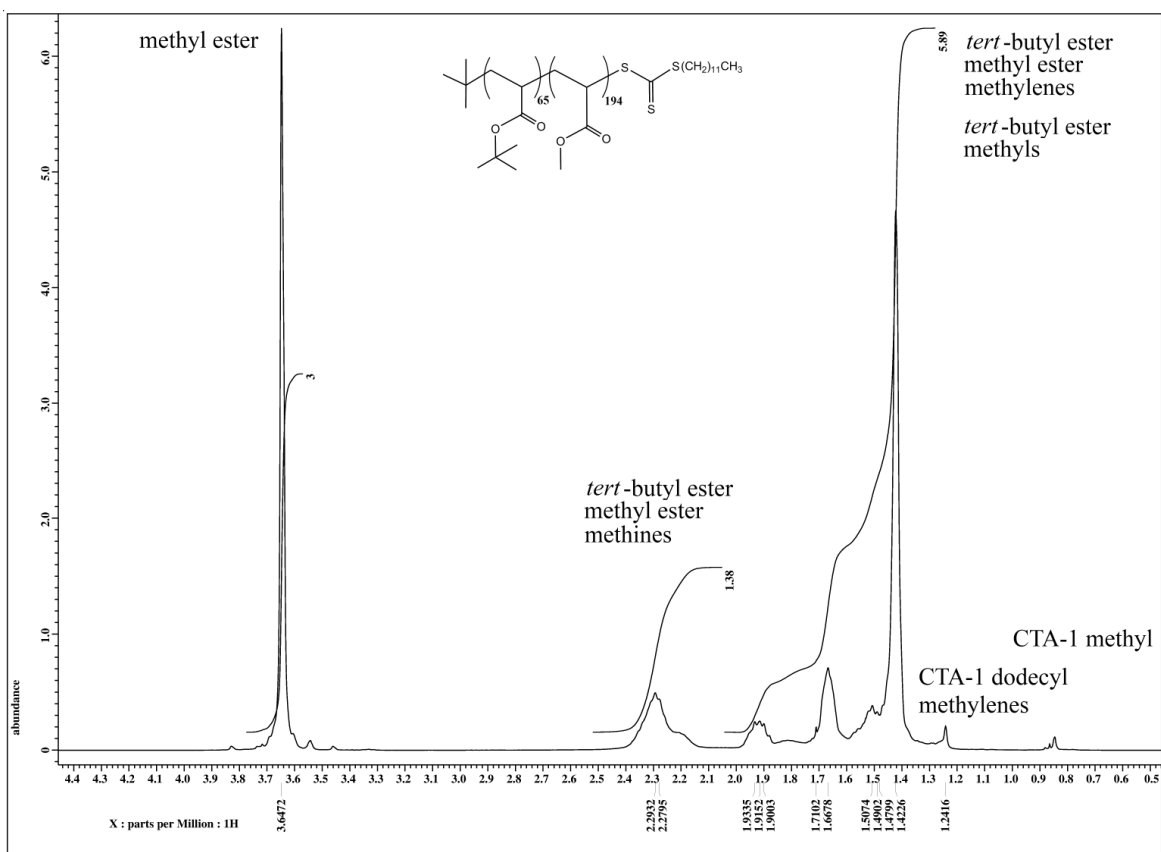


**Figure 13.** DTM-4 poly(*tert*-butyl acrylate-*b*-methyl acrylate) <sup>1</sup>H-NMR

## Poly(*tert*-butyl acrylate-*b*-methyl acrylate) $^{13}\text{C}$ -NMR

The  $^{13}\text{C}$ -NMR spectrum of poly(*tert*-butyl acrylate-*b*-methyl acrylate) contained ester carbonyl carbon peaks for both block types at 175.0 and 174.1 ppm. A methyl ester peak at 51.8 ppm also signified the presence of a second poly(methyl acrylate) block. Both methine resonances were present at 41.0-42.5 ppm, as indicated in Figure 14. The methylene region for DTM-4 had also broadened due to the incorporation of the second monomer with additional stereochemistry complexities of each block type. The *tert*-butyl ester  $4^\circ$  carbon and *tert*-butyl ester methyls present were previously identified in Figure 10.

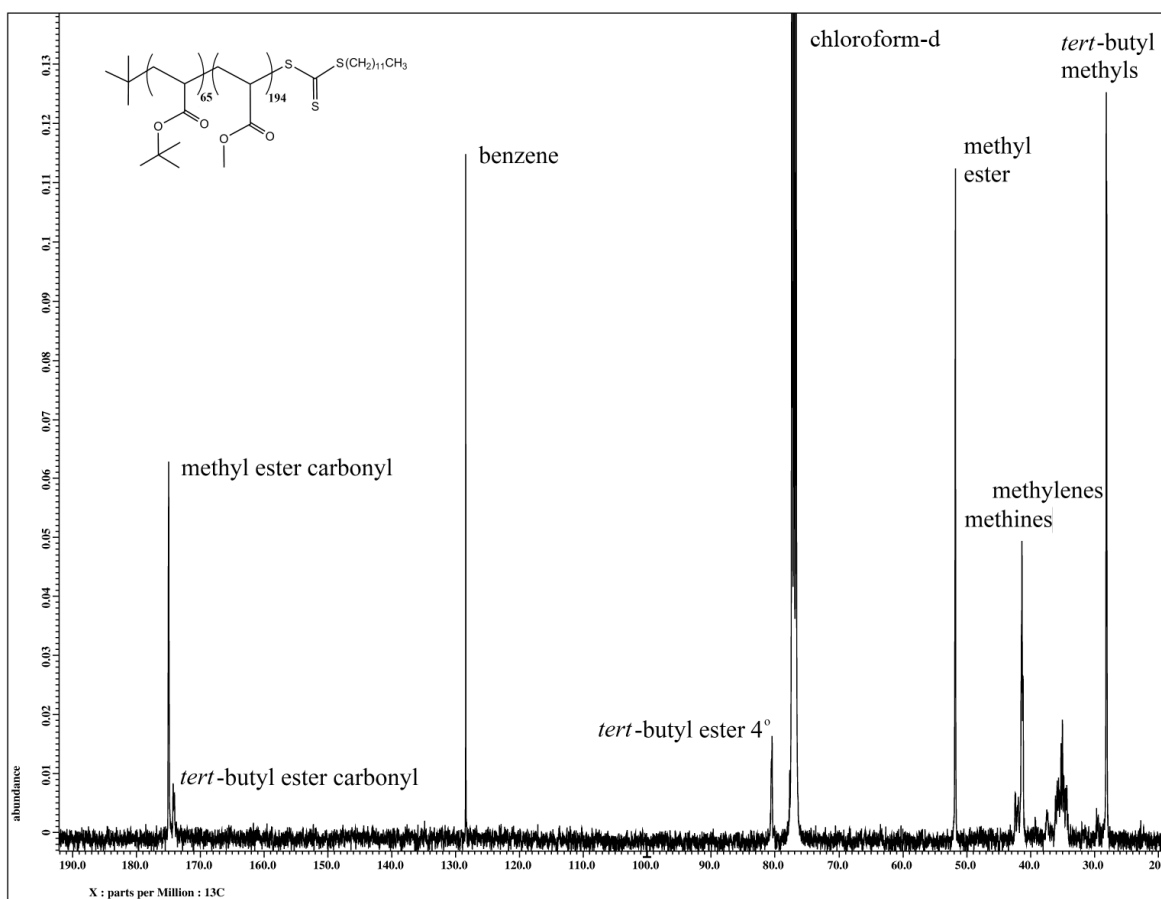


Figure 14. DTM-4 poly(*tert*-butyl acrylate-*b*-methyl acrylate)  $^{13}\text{C}$ -NMR

## Diblock Copolymer Percent Conversion $^1\text{H-NMR}$

In general, diblock copolymer percent conversion of the second block observed in  $^1\text{H-NMR}$  was higher when the  $D_p$  of the second block was low. DTM-5 poly(*tert*-butyl acrylate-*b*-methyl acrylate) (81-*b*-82) achieved 87.5% conversion of methyl acrylate to poly(methyl acrylate), whereas DTM-1 poly(*tert*-butyl acrylate-*b*-methyl acrylate) (198-*b*-439) experienced 74.6% conversion of the second monomer (Figure 15). Although other factors including monomer concentration, first block size, and block order also had an effect on monomer conversion for diblock copolymers, the second block size was a main factor in achieving high yield.

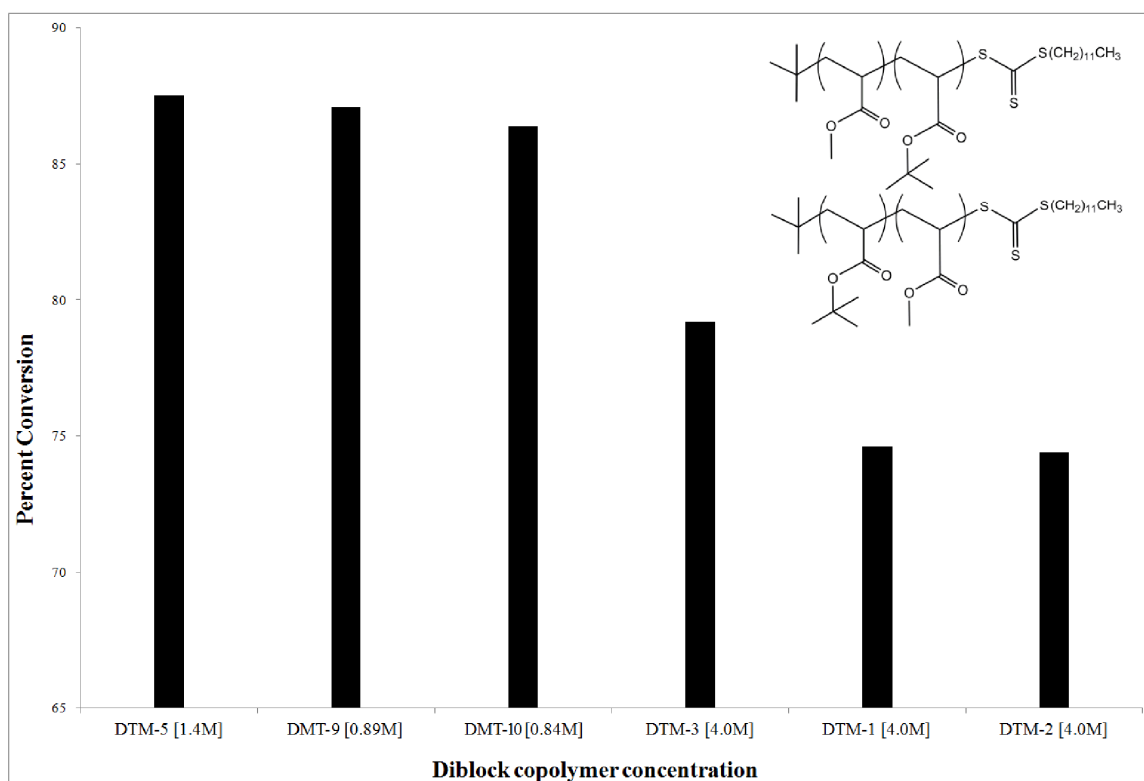
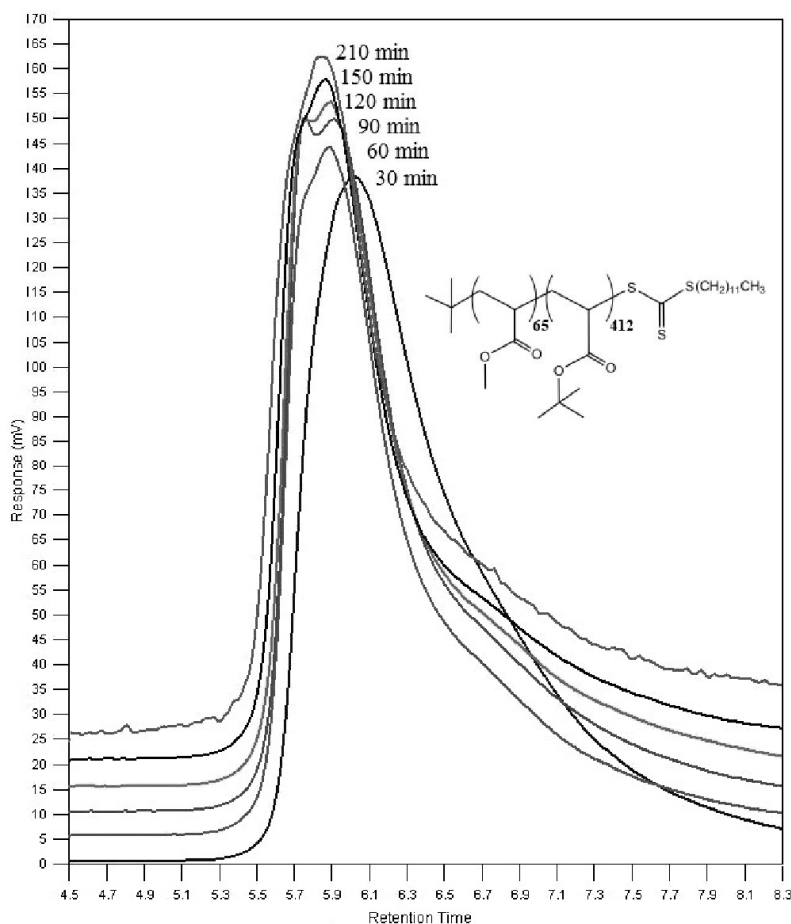


Figure 15. Diblock Percent Conversion Second Monomer  $^1\text{H-NMR}$

## Poly(methyl acrylate-*b*-*tert*-butyl acrylate) SEC

Molecular weight data as a function of polymerization time were collected on a poly(methyl acrylate-*b*-*tert*-butyl acrylate) sample with SEC, as depicted in Figure 16. As *tert*-butyl acrylate monomer was polymerized to the poly(*tert*-butyl acrylate) block, a bimodal distribution occurred between 60-120 min. The cause for separate molecular weight distributions was most likely equilibrating chain transfer processes. From 150 min to 210 min, the distribution for DMT-1 became monomodal again, which indicated that the diblock copolymer polymerization contained negligible amounts of poly(*tert*-butyl acrylate) from homopolymer side products at the end of the reaction.



**Figure 16.** DMT-1 poly(methyl acrylate-*b*-*tert*-butyl acrylate) SEC

### **Poly(acrylic acid-*b*-methyl acrylate) E-HSQC NMR**

The polymer and solvent  $^1\text{H}$ -NMR peaks of an amphiphilic poly(acrylic acid-*b*-methyl acrylate) copolymer sample dissolved in 25%  $\text{D}_2\text{O}$ /75% 1,4-dioxane- $\text{d}_8$  overlapped in the 3.5-3.6 ppm region. 2D correlations by E-HSQC NMR provided phasing information for methine (CH, green), methylene ( $\text{CH}_2$ , red), and methyl ( $\text{CH}_3$ , green) multiplicities, as annotated in Figure 17. The methyl ester peak at 3.59 ppm for DAC-1 was correlated to the 51.8 ppm  $^{13}\text{C}$ -NMR peak previously identified in Figure 14. A 1,4-dioxane peak identified as  $\text{CH}_2$  at 3.55 ppm correlated to a carbon singlet at 66.8 ppm. An additional 1,4-dioxane peak identified as CHD at 3.51 ppm correlated to a CD triplet at 66.2 ppm. The polymer methine protons at 2.25 ppm correlated to a carbon peak at 41.2 ppm; whereas the methylene protons at 1.63 ppm correlated to a 34.7 ppm broad carbon peak. Due to the overlap of the methyl ester and solvent protons, combined with uncertainty in the degree of deuteration of the 1,4-dioxane- $\text{d}_8$  solvent, an accurate integration of methyl ester to polymer back bone protons could not be made. However, the validation of polymer correlations and the lack of *tert*-butyl resonances by E-HSQC NMR assisted in confirming the presence of the DAC-1 product resonances.

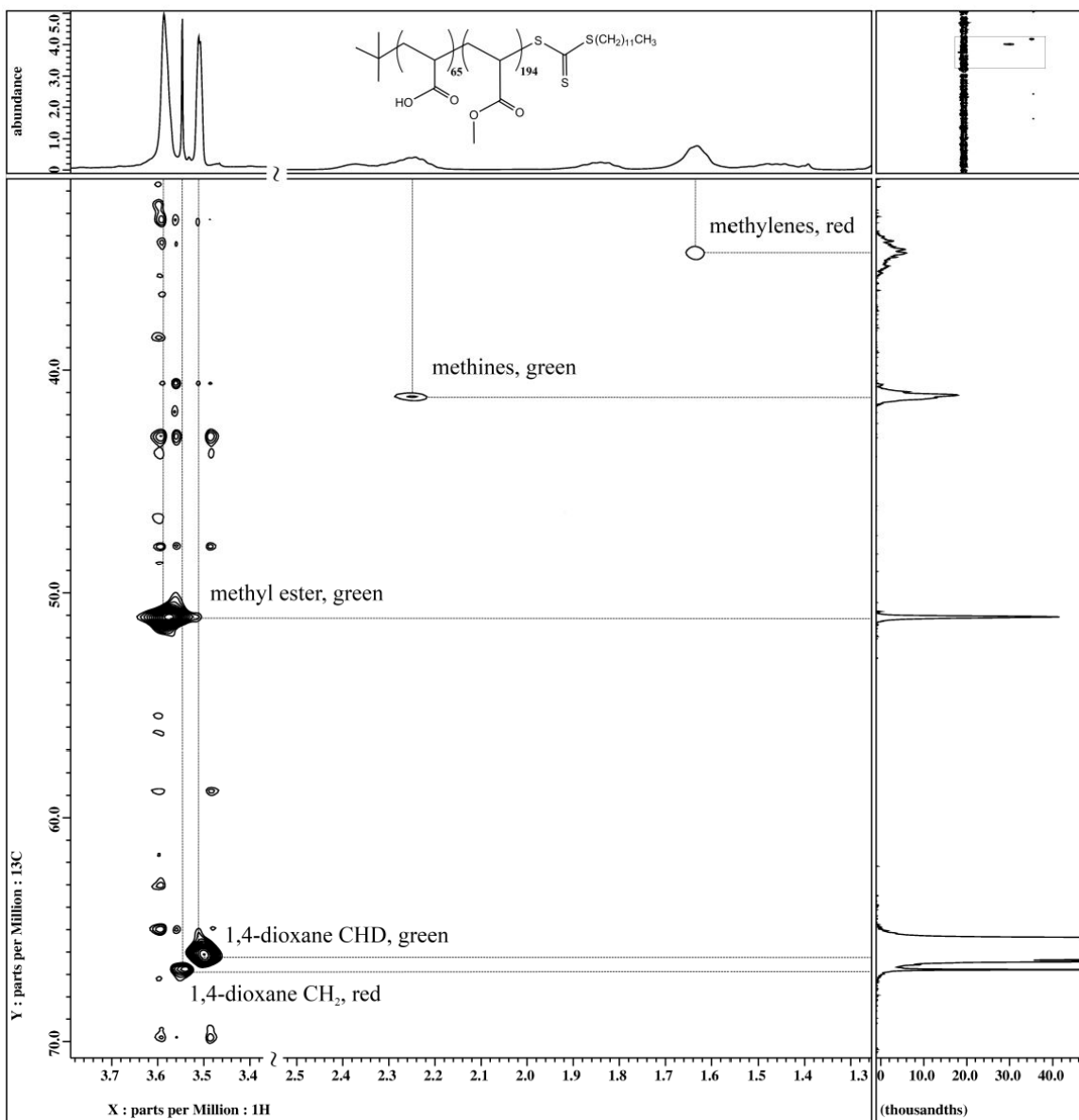


**Figure 17.** DAC-1 poly(acrylic acid-*b*-methyl acrylate) E-HSQC NMR



## Poly(acrylic acid-*b*-methyl acrylate) $^{13}\text{C}$ -NMR

The degree of polymerization for DAC-1 poly(acrylic acid-*b*-methyl acrylate) was verified by  $^{13}\text{C}$  carbonyl integration ratios. The carboxylic acid carbonyl:methyl ester carbonyl integration ratio of 1:3.15 in Figure 18 closely matched the theoretical poly(acrylic acid):poly(methyl acrylate) ratio of 1:2.98, or 65:194. The  $^{13}\text{C}$  carbonyl integrations of DAC-1 were not affected by nuclear Overhauser effect (NOE) enhancement, and were considered accurate approximations without accounting for  $T_1$  diffusion and long relaxation delays typical of long polymer chains. Thus,  $^{13}\text{C}$  integrations provided a validation of monomer:CTA and second monomer: homopolymer ratios despite the inability to confirm poly(acrylic acid) blocks using SEC.

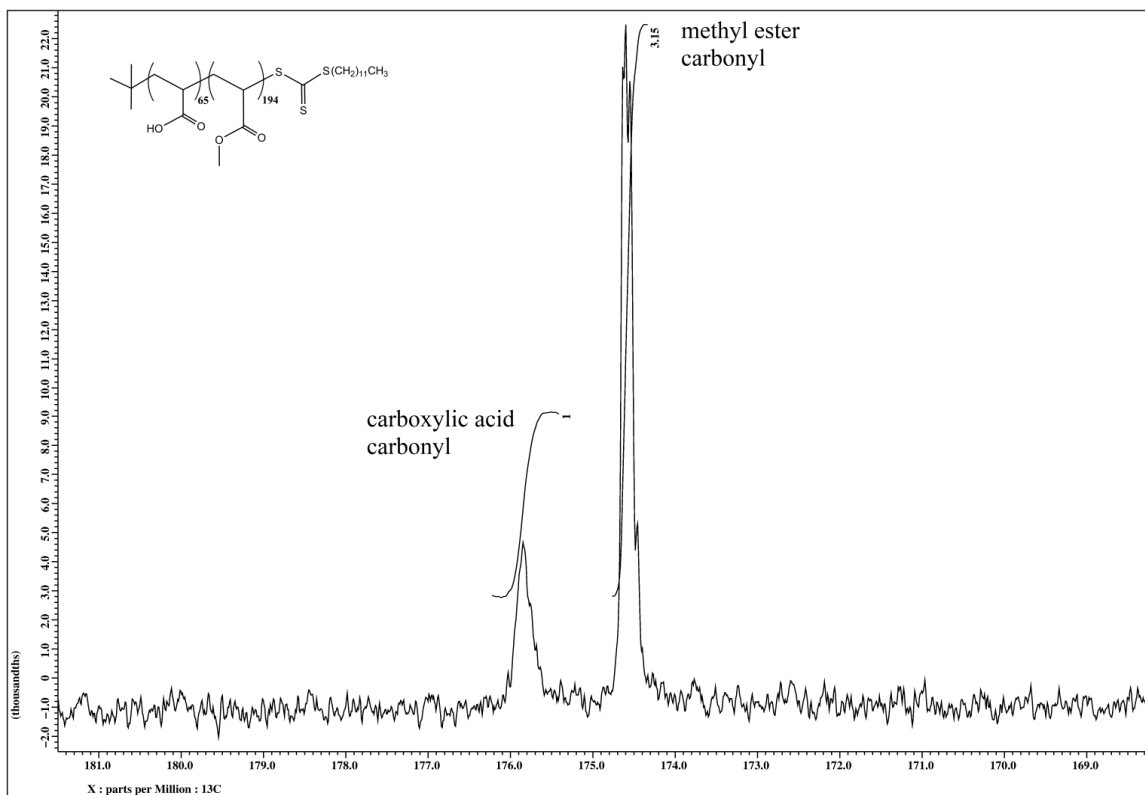


**Figure 18.** DAC-1 poly(acrylic acid-*b*-methyl acrylate)  $^{13}\text{C}$ -NMR

## Poly(methyl acrylate-*b*-acrylic acid) (66-*b*-60) <sup>1</sup>H-NMR

Previous findings by Wilmes et al. of a poly(methyl acrylate-*b*-acrylic acid) (66-*b*-60) (SEC-<sup>1</sup>H-NMR) suggested that the polymer did not form micelles in solutions of D<sub>2</sub>O and 1,4-dioxane-*d*<sub>8</sub>.<sup>18</sup> Copolymer containing a more rigid poly(methyl methacrylate) block did show evidence of micellization in <sup>1</sup>H-NMR at moderate concentrations of D<sub>2</sub>O. The hypothesis of chain rigidity assisting the hydrophobic block's ability to form micelle structures was verified with a low molecular weight, flexible acrylate block failing to produce micelles. The negligible coalescence of the methine peaks from the less rigid poly(methyl acrylate) and poly(acrylic acid) blocks in 50%/50% and 75%/25% D<sub>2</sub>O/1,4-dioxane-*d*<sub>8</sub> mixtures was taken as evidence that micellization did not occur for DMA-6 in the presence of D<sub>2</sub>O (Figure 19).

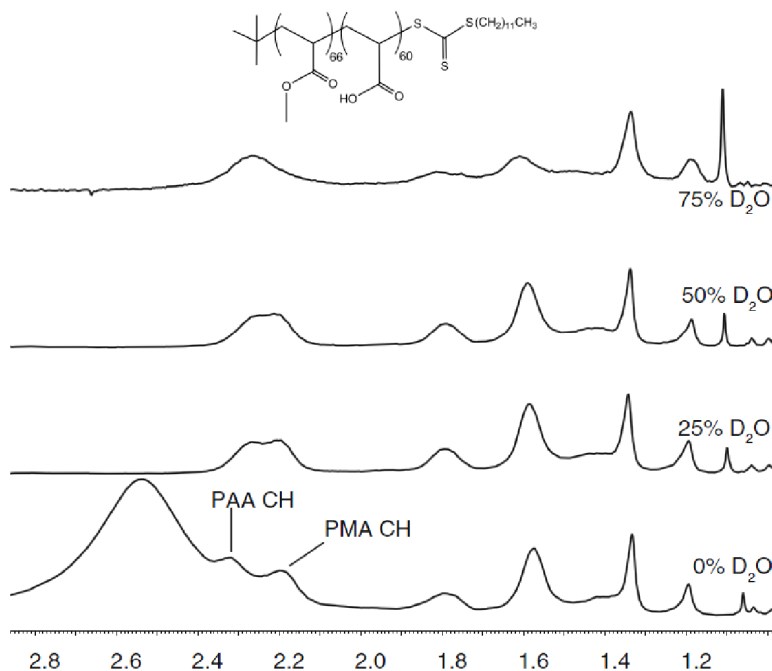


**Figure 19.** DMA-6 poly(methyl acrylate-*b*-acrylic acid) (66-*b*-60) <sup>1</sup>H-NMR

### **Poly(acrylic acid-*b*-methyl acrylate) (65-*b*-194) <sup>1</sup>H-NMR**

A poly(acrylic acid-*b*-methyl acrylate) (65-*b*-194) copolymer consisting of a longer hydrophobic block than used in chain rigidity experiments was observed in <sup>1</sup>H-NMR for effects of micellization (Figures 20 and 21). The DAC-1 sample in 25% D<sub>2</sub>O/75% 1,4-dioxane-d<sub>8</sub>, with a benzene standard, displayed a prominent methyl ester peak at 3.54 ppm. The poly(acrylic acid) and poly(methyl acrylate) methine peaks at 2.1-2.4 ppm were also prominent. In the 75% D<sub>2</sub>O/25% 1,4-dioxane-d<sub>8</sub> sample, the methyl ester resonance was 2.4 times less prominent than in the 25% D<sub>2</sub>O sample. The 1,4-dioxane solvent peak identified in the 75% D<sub>2</sub>O sample was smaller due to its lower concentration in the aqueous solution previously identified in Figure 17. The methine region in the 75% D<sub>2</sub>O sample was 5.4 times less prominent than in the non-micellar, more hydrophobic solution.

In NMR micellization experiments, the presence of diminished hydrophobic block proton resonances may indicate that aggregated molecular structures did form. By incorporating a poly(methyl acrylate) block in DAC-1 that was roughly three times as large as in DMA-6, additional hydrophobic interactions of the lengthened hydrophobic block appear to have caused micelle formation in an aqueous environment, which led to a decrease in proton integrations. In addition, when DAC-1 was introduced to the 75% D<sub>2</sub>O environment, the presence of a viscous cloudy suspension in solution was observed. Conversely, positive <sup>1</sup>H-NMR results and physical characteristics typical of micelle formation could still indicate that some other non-micellar structure was formed. Additional analysis with T<sub>1</sub>/T<sub>2</sub> relaxation experiments and light scattering methods may help to further improve the certainty of micelle existence and size in future experiments.

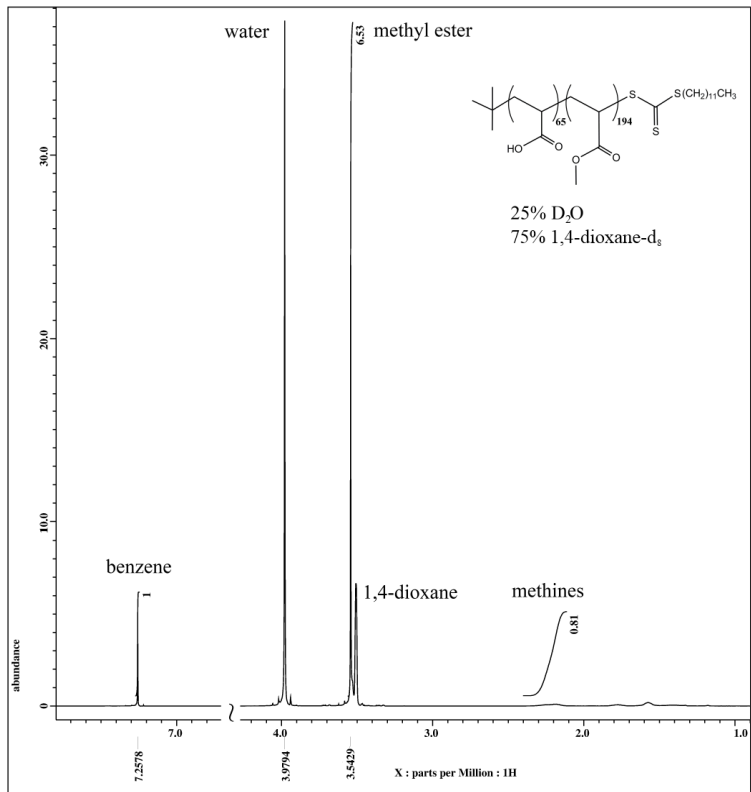


Figure 20. DAC-1 poly(acrylic acid-*b*-methyl acrylate) (65-*b*-194) 25% D<sub>2</sub>O <sup>1</sup>H-NMR

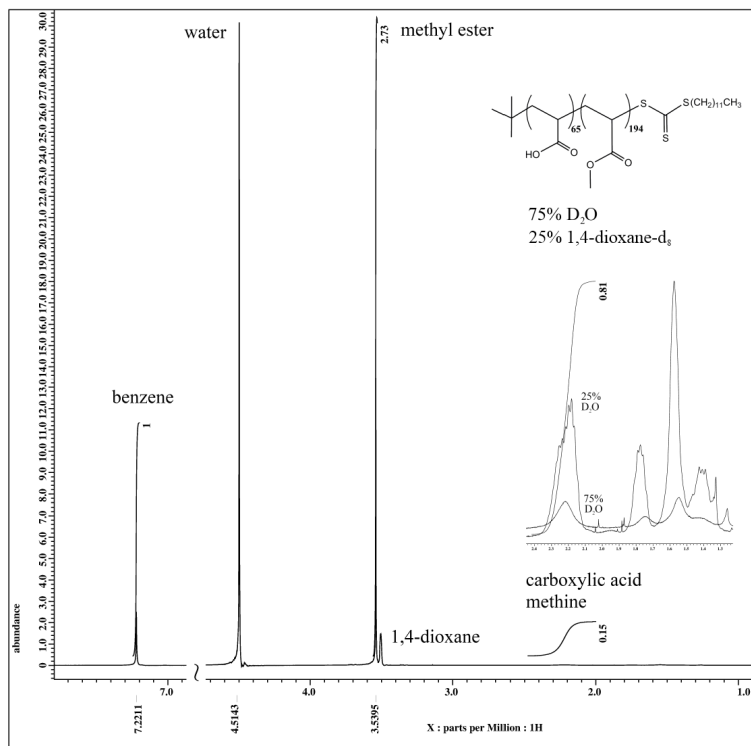


Figure 21. DAC-1 poly(acrylic acid-*b*-methyl acrylate) (65-*b*-194) 75% D<sub>2</sub>O <sup>1</sup>H-NMR

## Chapter 4: Conclusions

Amphiphilic diblock copolymers show promise as micellar transport devices of hydrophobic drugs such as cisplatin and doxorubicin. When these polymers are introduced into an aqueous environment, a protective core-shell complex can form around the hydrophobic species. Reversible addition fragmentation chain transfer (RAFT) is a radical chain growth polymerization method that uses equilibrium and transfer processes to yield a narrow distribution of polymer molecular weights. Production of monodisperse RAFT polymers is desirable due to their predictable thermodynamic properties appropriate for use in medicinal transport systems.  $^1\text{H-NMR}$  and  $^{13}\text{C-NMR}$  (Nuclear Magnetic Resonance) spectroscopy was used in verifying chain transfer agent (CTA) products and detecting polymerization in experiments. Consumption of monomer proceeded rapidly for homopolymers, whereas diblock copolymer formation was slightly less effective in converting 75-85% of monomer. Increasing the polymer molecular weight generally decreased monomer conversion. RAFT polymer growth rates obtained by size exclusion chromatography (SEC) depicted a gradual increase of molecular weight with reaction time and reflected the monomer:CTA ratio upon exhaustion of the monomer.

The 2D E-HSQC (Edited-Heteronuclear Single Quantum Correlation) NMR method was used to assign amphiphilic copolymer and solvent peaks, which was necessary for characterizing  $^1\text{H}$  resonances in micellization experiments. A main factor that appeared to affect micellization of acrylate-based amphiphilic block copolymers was chain length. A relatively short hydrophobic poly(methyl acrylate) block of poly(methyl acrylate-*b*-acrylic acid) (66-*b*-60) failed to display the effects of micellization in an aqueous environment when compared to a sample with a hydrophobic block that was about three times as large.

The effects of micellization were observed when the lengthened poly(methyl acrylate) block  $^1\text{H}$  resonances of poly(acrylic acid-*b*-methyl acrylate) were diminished when the solvent hydrophilicity was increased to 75%  $\text{D}_2\text{O}$ . The experimental results reflected the hypothesis of the study summarized by the hydrophobic block collapse theory, in which hydrophobic forces of additional methyl acrylate repeat units assisted in forming an aqueous micelle solution. Further experimentation with acrylate-based amphiphilic diblock copolymers using light scattering or other spectroscopic techniques may assist in ultimately addressing the issue of drug precipitation in the body.

## References

1. Kwon, G.; Naito, M.; Yokoyama, M.; Okano, T.; Sakurai, Y., Kataoka, K. Micelles Based on AB Block Copolymers of Poly(ethylene oxide) and Poly( $\beta$ -benzyl L-aspartate). *Langmuir*. **1993**, *9*, 945-949.
2. Perrier, S.; Takolpuckdee, P.; Mars, C. A. Reversible Addition-Fragmentation Chain Transfer Polymerization: End Group Modification for Functionalized Polymers and Chain Transfer Agent Recovery. *Macromolecules*. **2005**, *38*, 2033-2036.
3. Bader, H.; Ringsdorf, H.; Schmidt, B. Water soluble polymers in medicine. *Ang. Makromol. Chem.* **1984**, *123*, 457-485.
4. Kataoka, K.; Harada, A.; Nagasaki, Y. Block Copolymer micelles for drug delivery: design, characterization and biological significance. *Adv. Drug Deliver Rev.* **2001**, *47*, 113-131.
5. Mukerjee, P.; Mysels, K. J. *Critical Micelle Concentrations of Aqueous Surfactant Systems*; ADD095344; DTIC: 1971.
6. Robson, R. J.; Dennis, E. A. The Size, Shape, and Hydration of Nonionic Surfactant Micelles. Triton X-100. *J. Phys. Chem.* **1977**, *81*, 1075-1078.
7. Cabane, B.; Duplessix, R. Organization of surfactant micelles adsorbed on a polymer molecule in water; a neutron scattering study. *J. Physique*. **1982**, *43*, 1529-1542.
8. Kile, D. E.; Chiou, C. T. Water Solubility Enhancements of DDT and Trichlorobenzene by Some Surfactants Below and Above the Critical Micelle Concentration. *Environ. Sci. Technol.* **1989**, *23*, 832-838.
9. Jain, N.; Trabelsi, S.; Guillot, S.; McLoughlin, D.; Langevin, D.; Letellier, P.; Turmine, M. Critical Aggregation Concentration in Mixed Solutions of Anionic Polyelectrolytes and Cationic Surfactants. *Langmuir*. **2004**, *20*, 8496-8503.

10. Holmberg, K.; Jonsson, B.; Kronberg, B.; Lindman, B. Intermolecular Interactions. In *Surfactants and Polymers in Aqueous Solution*; Ed.; Wiley: England, 2003, p 157.
11. Kataoka, K.; Ishihara, A.; Harada, A.; Miyazaki, H. Effect of secondary structure of poly(L-Lysine) segments on the micellization of poly(ethylene glycol)-poly(L-Lysine) block copolymer partially substituted with hydrocinnamoyl-group at the N<sup>α</sup>-position in aqueous milieu. *Macromolecules*. **1998**, *31*, 6071-6076.
12. Kabanov, A. V.; Vinogradov, S. V.; Suzdaltseva, Y. G.; Suzdaltseva, V. Y.; Alakhov, V. Y. Water soluble block polycations as carriers for oligonucleotide delivery. *Bioconjug. Chem.* **1995**, *6*, 639-643.
13. Yu, Z.; Zhao, G. The physicochemical properties of aqueous mixtures of cationic-anionic surfactants: II. Micelle growth pattern of equimolar mixtures. *J. Colloid Interface Sci.* **1989**, *130*, 421-431.
14. Lam, Y. M.; Goldbeck-Wood, G. Mesoscale simulation of block copolymers in aqueous solution: parameterisation, micelle growth kinetics and the effect of temperature and concentration morphology. *Polymer*. **2003**, *44*, 3593-3605.
15. Schmaljohann, D. Thermo- and pH-responsive polymers in drug delivery. *Adv. Drug. Deliv. Rev.* **2006**, *58*, 1655-1670.
16. Chung, J. E.; Yokoyama, M.; Yamato, M.; Aoyagi, T.; Sakurai, Y.; Okano, T. Thermo-responsive drug delivery from polymeric micelles constructed using block copolymers of poly(*N*-isopropylacrylamide) and poly(butylmethacrylate). *J. Control. Release*. **1999**, *62*, 115-127.



17. Hosoya, K.; Yoshizako, K.; Kubo, T.; Ikegami, T.; Tanaka, N.; Haginaka, J. Selective Surface Modification Technique for Improvement of Chromatographic Separation Selectivity for Sugar Derivatives. *Anal. Sci.* **2002**, *18*, 55-58.
18. Wilmes, G. M.; Arnold, D. J.; Kawchak, K. S. Effect of chain rigidity on block copolymer micelle formation and dissolution as observed by <sup>1</sup>H-NMR spectroscopy. *J. Polym. Res.* **2011**, *18*, 1787-1797.
19. Kim, Y.; Pourgholami, M. H.; Morris, D. L.; Stenzel, M. H. Effect of Cross-Linking on the Performance of Micelles As Drug Delivery Carriers: A Cell Uptake Study. *Biomacromolecules.* **2012**.
20. Trubetsky, V. S.; Torchilin, V. P. Polyethyleneglycol based micelles as carriers of therapeutic and diagnostic agents. *STP Pharma. Sci.* **1996**, *6*, 79-86.
21. Nakanishi, T.; Fukushima, A.; Okamoto, K.; Suzuki, M.; Matsumura, Y.; Yokoyama, M.; Okano, T.; Sakurai, Y.; Kataoka, K. Development of the polymer micelle carrier system for doxorubicin. *J. Control. Release.* **2001**, *74*, 295-302.
22. Kabanov, A. V.; Batrakova, E. V.; Alakhov, V. Y. Pluronic® block copolymers as novel polymer therapeutics for drug and gene delivery. *J. Control. Release.* **2002**, *82*, 189-212.
23. Yasugi, K.; Nakamura, T.; Nagasaki, Y.; Kato, M.; Kataoka, K. Sugar installed polymer micelles: Synthesis and micellization of poly(ethylene glycol)-poly(D,L-lactide) block copolymers having sugar groups at the PEG chain end. *Macromolecules.* **1999**, *32*, 8024-8032.
24. Scholz, C.; Iijima, M.; Nagasaki, Y.; Kataoka, K. A Novel Reactive Polymeric Micelle with Aldehyde Groups on Its Surface. *Macromolecules.* **1995**, *28*, 7295-7297.

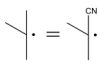
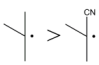
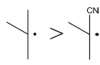
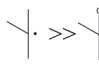
25. Masayuki, Y.; Mizue, M.; Noriko, Y.; Teruo, O.; Yasuhisa, S.; Kazunori, K.; Shohei, I. Polymer micelles as novel drug carrier: Adriamycin-conjugated poly(ethylene glycol)-poly(aspartic acid) block copolymer. *J. Control. Release.* **1990**, *11*, 269-278.
26. Yokoyama, M. et al. Characterization and Anticancer Activity of the Micelle-forming Polymeric Anticancer Drug Adriamycin-conjugated Poly(ethylene glycol)-Poly(aspartic acid) Block Copolymer. *Cancer Res.* **1990**, *50*, 1693-1700.
27. Yokoyama, M.; Okano, Y.; Sakurai, Y. Suwa, S.; Kataoka, K. Introduction of cisplatin into polymeric micelle. *J. Control. Release.* **1996**, *39*, 351-356.
28. Nishiyama, N.; Yokoyama, M.; Aoyagi, T.; Okano, T.; Sakurai, Y.; Kataoka, K. Preparation and characterization of self-assembled polymer-metal complex micelle from cis-dichlorodiamine platinum (II) and poly(ethylene glycol)-poly( $\alpha,\beta$ -aspartic acid) block copolymer in an aqueous medium. *Langmuir.* **1999**, *15*, 377-383.
29. Kwon, G. S.; Naito, M.; Yokoyama, M.; Okano, T.; Sakurai, Y.; Kataoka, K. Physical entrapment of Adriamycin in AB block copolymer micelles, *Pharm. Res.* **1995**, *12*, 192-195.
30. Bazile, D.; Prud'homme, C.; Bassoulet, M.; Marland, M.; Spenlehauer, G.; Veillard, M. Stealth Me.PEG-PLA nanoparticles avoid uptake by the mononuclear phagocytes system. *J. Pharm. Sci.* **1995**, *84*, 493-498.
31. Chiefari, J.; Chong, Y. K.; Ercole, F.; Kirstina, J.; Jeffery, J.; Le, T. P. T.; Roshan, T.; Mayadunne, A.; Meijs, G. F.; Moad, C. L.; Moad, G.; Rizzardo, E.; Thang, S. H. Living Free Radical Polymerization by Reversible Addition-Fragmentation Chain Transfer: The RAFT Process. *Macromolecules.* **1998**, *31*, 5559-5562.

32. Donovan, M. S.; Lowe, A. B.; Sumerlin, B. S.; McCormick, C. L. Raft Polymerization of *N,N*-Dimethylacrylamide Utilizing Novel Chain Transfer Agent Tailored for High Reinitiation Efficiency and Structural Control. *Macromolecules*. **2002**, *35*, 4123-4132.
33. Barner-Kowollik, C.; Coote, M. L.; Davis, T. P.; Radom, L. The Reversible Addition-Fragmentation Chain Transfer Process and the Strength and Limitations of Modeling: Comment on "The Magnitude of the Fragmentation Rate Coefficient". *J. Polym. Sci.* **2003**, *41*, 2828-2832.
34. Colombani, O.; Langelier, O.; Martwong, E. Polymerization Kinetics: Monitoring Monomer Conversion Using an Internal Standard and the Key Role of Sample  $t_0$ . *J. Chem. Educ.* **2011**, *88*, 116-121.
35. Moad, G.; Rizzardo, E.; Thang, S. H. Living Radical Polymerization by the RAFT Process. *Aust. J. Chem.* **2005**, *58*, 379-410.
36. Luo, Y.; Wang, R.; Yang, L.; Yu, B.; Li, Bogeng; Zhu, S. Effect of Reversible Addition – Fragmentation Transfer (RAFT) Reactions on (Mini)emulsion Polymerization Kinetics and Estimate of RAFT Equilibrium Constant. *Macromolecules*. **2006**, *39*, 1328-1337.
37. Convertline, A. J.; Lokitz, B. S.; Vasileva, Y.; Myrick, L. J.; Scales, C. W.; Lowe, A. B.; McCormick, C. L. Direct Synthesis of Thermally Responsive DMA/NIPAM Diblock and DMA/NIPAM/DMA Triblock Copolymers via Aqueous, Room Temperature RAFT Polymerization. *Macromolecules*. **2006**, *39*, 1724-1730.
38. Sumerlin, B. S.; Lowe, A. B.; Thomas, D. B.; McCormick, C. L. Aqueous Solution Properties of pH-Responsive AB Diblock Acrylamido Copolymers Synthesized via Aqueous RAFT. *Macromolecules*. **2003**, *36*, 5982-5987.

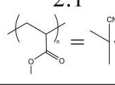
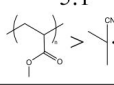
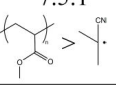
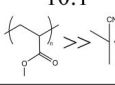
39. Eberhardt, M.; Theato, P. RAFT Polymerization of Pentafluorophenyl Methacrylate: Preparation of Reactive Linear Diblock Copolymers. *Macromol. Rapid Comm.* **2005**, *26*, 1488-1493.
40. Hou, S.; Chaikof, E. L.; Taton, D.; Gnanou, Y. Synthesis of Water-Soluble Star-Block and Dendrimer-like Copolymers Based on Poly(ethylene oxide) and Poly(acrylic acid). *Macromolecules.* **2003**, *36*, 3874-3881.
41. Cai-Yuan, P.; Chun-Yan, H. Synthesis and Characterizations of Block Copolymers Prepared via Controlled Radical Polymerization Methods. In *Developments in Block Copolymer Science and Technology*; Hamley, I. W., Ed.; Wiley: England, 2004, p 199.
42. York, A. W.; Kirkland, S. E.; McCormick, C. L. Advances in the synthesis of amphiphilic block copolymers via RAFT polymerization: Stimuli-responsive drug and gene delivery. *Adv. Drug Deliv. Rev.* **2008**, *60*, 1018-1036.
43. McGraw-Hill: Chapter 20: Carboxylic Acid Derivatives. Nucleophilic Acyl Substitution. <http://www.mhhe.com/physsci/chemistry/carey/student/olc/ch20reactionsnitriles.html> (accessed Aug 23, 2011).
44. Smith, J. G. *Organic Chemistry*, 2nd ed.; McGraw-Hill: New York, 2007.
45. Kiani, K.; Hill, D. J. T.; Rasoul, F.; Whittaker, M.; Rintoul, L. Raft Mediated Surface Grafting of *t*-Butyl Acrylate onto an Ethylene-Propylene Copolymer Initiated by Gamma Radiation. *J. Polym. Sci. Part A: Poly. Chem.* **2007**, *45*, 1074-1083.
46. Whittaker, M. R.; Monteiro, M. J. Synthesis and Aggregation Behavior of Four-Arm Star Amphiphilic Block Copolymers in Water. *Langmuir.* **2006**, *22*, 9746-9752.

47. Abraham, S.; Kim, C. H. Synthesis of poly(styrene-*block-tert*-butyl acrylate) star polymers by atom transfer radical polymerization and micellization of their hydrolyzed polymers. *J. Polym. Sci., Part A: Polym. Chem.* **2005**, *43*, 6367-6378.
48. Skey, J.; O'Reilly, R. K. Facile one pot synthesis of a range of reversible addition-fragmentation chain transfer (RAFT) agents. *Chem. Commun.* **2008**, *35*, 4183-4185.
49. Smith, A. E.; Xu, X.; McCormick, C. L. Stimuli-responsive amphiphilic (co)polymers via RAFT polymerization. *Prog. Polym. Sci.* **2010**, *35*, 45-93.
50. Bromberg, L.; Temchenko, M.; Hatton, T. A. Dually Responsive Microgels from Polyether-Modified Poly(acrylic acid): Swelling and Drug Loading. *Langmuir.* **2002**, *18*, 4944-4952.
51. Silverstein, R. M.; Webster, F. X.; Kiemle, D. J. *Spectrometric Identification of Organic Compound*, 7th ed.; Wiley: Hoboken, 2005.
52. Wu, T.K.; Ovenall, D. W. Proton and Carbon-13 Nuclear Magnetic Resonance Studies of Poly(vinyl alcohol). *Macromolecules.* **1973**, *6*, 582-584.
53. Yau, W. W.; Kirkland, J. J.; Bly, D. D. Modern size-exclusion liquid chromatography: *Practice of gel permeation and gel filtration chromatography*. Wiley: New York, 1979.
54. Barth, H. G.; Mays, J. W. *Modern Methods of polymer characterization*: Wiley: New York, 1991.
55. Safir, A. L.; Novak, B. M. Living 1,2-Olefin-Insertion Polymerizations Initiated by Palladium(II) Alkyl Complexes: Block Copolymers and a Route to Polyacetylene-Hydrocarbon Diblocks. *Macromolecules.* **1995**, *28*, 5396-5398.

## Appendix A

Homopolymer Variables			
[Monomer]			
1M Non-Viscous Slow	2M	3M	4M Viscous Fast
Monomer:CTA			
50:1 Non-Viscous	100:1	150:1	200:1 Viscous
CTA:AIBN			
2:1 	5:1 	7.5:1 	10:1 
Conditions			
Volume, Temperature, Time			
Purifications			
Reduced Pressure, Precipitation			

## Appendix B

Diblock Copolymer Variables			
[2nd Monomer]			
1M Non-Viscous Slow	2M	3M	4M Viscous Fast
2nd Monomer:Homopolymer			
50:1 Non-Viscous	100:1	150:1	200:1 Viscous
Homopolymer:AIBN			
2:1 	5:1 	7.5:1 	10:1 
Conditions			
Volume, Temperature, Time			
Purifications			
Reduced Pressure, Precipitation			